JOURNAL OF GEOPHYSICAL RESEARCH, VOL. 97, NO. C9, PAGES 14,453–14,474, SEPTEMBER 15, 1992

Assimilation of Altimeter Data in a Global Third-Generation Wave Model

P. LIONELLO[1] AND H. GÜNTHER[2]

European Centre for Medium Range Weather Forecasts, Reading, England

P. A. E. M. JANSSEN

Royal Netherlands Meteorological Institute, De Bilt

We investigated the effect of the assimilation of altimeter satellite data in the third-generation ocean wave model WAM. We used a sequential method, where analyzed significant wave height fields are created by optimum interpolation, and the analyzed values are then used to construct the analyzed wave spectrum. The method provides also an estimate of the surface stress showing the possibility of using the analysis of the wave spectrum to derive an analyzed surface stress field. In a first set of numerical experiments, the data, provided by the Seasat altimeter, have been assimilated in the WAM model for $1\frac{1}{2}$ days. The comparison between model results and satellite data during the continuation of the run shows a positive and persistent impact of the assimilation. In a second set of numerical experiments, Geosat altimeter data were assimilated for 10 days and the resulting analysis was compared with buoy data. Although the assimilation improves the model results, it is not capable of compensating the differences between model and buoys. Some failures are clearly derived from the absence in the satellite data of the high-wave events that were reported by the buoys. Other failures may be the consequence of an excessive swell attenuation in the WAM model, which compromises the effect of a previous correction. In fact, the comparison of WAM model results with altimeter data suggests that there is a tendency of the model to overevaluate initially the wind sea, and successively to overestimate the decay of the wave energy, when the waves leave the area of the storm.

1. INTRODUCTION

The launch of oceanographic satellites has provided wind wave modelers with a new and extensive set of measurements, which represents a remarkable change with respect to the previous situation when few measurements were available in scattered locations corresponding to platforms, buoys, and oceanographic ships. The assimilation of so few data was not object of much attention in wave modeling, substantially because it was not necessary to produce a reliable description of the wave field. In fact, in contrast to weather forecasting, wave forecasting is in many aspects a boundary value problem and not an initial value problem; the wave field tends to lose the memory of the initial state, and its description benefits from the assimilation that has been performed in the atmospheric model which produced the driving wind fields. The purpose of data assimilation is therefore to correct the model and to produce a better performance, but it is not a necessary part of a wave prediction system. While the impact of the few data available in the past was not expected to be very relevant on a global scale, the wide coverage produced by satellite measurements is expected to have a substantial effect.

The improvement of the wave forecast is not the only reason to analyze the wave measurements; another motivation is that owing to the dependence of the wave model results on the surface stress field, a coupled wind and wave assimilation can improve the performance of the atmospheric model, supplying further information on the stress field. In fact ocean waves can be categorized as wind sea or swell, the first term denoting waves that are evolving under the action of the wind and the second denoting waves that are freely propagating, the wind being too weak to affect them. This study actually shows how an evaluation of the surface stress can be derived by the analysis of the wave model results, producing a consistent analysis of the wave spectrum and the surface stress where there is wind sea. On the other hand, the consistent modification of surface stress and wave spectrum is a necessary requirement of a wave assimilation scheme; in fact, the updating of the wind sea has a little effect unless the surface stress is also updated, because the correction would otherwise be erased by the incorrect wind forcing.

The practical target of this study is to develop a system that could use satellite data in an operational framework, i.e., a tool that could be used, for a regular, daily assimilation of satellite data with limited computer resource costs, ready for the ERS-1 mission.

Two devices will be mounted on ERS-1 which will provide information on the wind waves: the altimeter and the synthetic aperture radar (SAR). The altimeter provides measurements of the significant wave height (SWH) along the satellite track with good accuracy (0.5 m or 10% of SWH, whichever is larger). The measurement is based on the modification in the rise time produced by the wavy surface in the backscattered signal. The result is interpreted as SWH. Potentially much more information is contained in the SAR images, from which the wave spectrum can be deduced. Unfortunately the transfer from SAR image to wave spectrum is not a one-to-one mapping; waves may not be detected owing to excessive noise or to high nonlinearity. The picture of the sea surface is distorted, and the distortion

[1]Now at Istituto per lo Studio della Dinamica delle Grandi Masse, Consiglio Nazionale delle Ricerche, Venice, Italy.

[2]Permanently at Forschungszentrum GKSS, Geesthacht, Germany.

Paper number 92JC01055.
0148-0227/92/92JC-01055$05.00

depends on the component of the velocity of the waves normal to the satellite flight direction. It is then not isotropic. Because of these problems a first-guess spectrum must be provided by a wave model to interpret adequately the SAR image. A procedure to produce in most of the cases an analyzed spectrum is actually available [*Brüning et al.*, 1990], and it has been applied to Seasat data. Unfortunately, a very limited number of spectra have been produced to date, and they are not enough to study the impact of SAR on the wave prediction. No SAR was mounted on Geosat. Therefore as no routine inversion of the SAR image was available by the beginning of this study, we sought a method that could analyze the wave field without the need of wave spectra measurements. Although this method could be readily extended to use peak frequency and peak direction which could be provided by SAR, only altimeter data have been used.

At present, for wave assimilation, as for assimilation in circulation models, there are two main classes of assimilation methods: sequential methods and variational methods. Sequential methods perform a series of N independent corrections, each at a different time $t_i (i = 1, \cdots, N)$, each time using the observations available in a time window centered at the time t_i. At each assimilation time t_i, the wave field is modified to agree as much as possible with observations, taking into account the reliability of both model results and measurements. In this respect they may be called single time level schemes. The sequence of fields is not consistent with the model dynamics, a discontinuity in the development being introduced at every assimilation time t_i.

Variational methods aim to find the model solution which minimizes the differences with observations over the whole analysis period by introducing corrections in the sequence of wind fields driving the wave model. In this respect they are also called multiple time level schemes. As the wave model equations are used as constraint, the process produces a sequence of wave fields which are at every time step consistent with the wave model dynamics. Note that the sequence of analyzed wind fields will not be in general consistent with the dynamics of the atmospheric model, unless the atmospheric model itself is also involved in the analysis. At present, practical difficulties and enormous costs prevent this solution. The quantity to minimize is the cost function

$$\Upsilon = \Upsilon_{wa} + \Upsilon_{wi} \tag{1}$$

$$\Upsilon_{wa} = \sum_{i=1}^{N_{\text{obs}}} (a_P^i - a_O^i) A_{ij} (a_P^j - a_O^j) \tag{2}$$

$$\Upsilon_{wi} = \Upsilon_{wi}(\bar{b}) \tag{3}$$

The a_P^i denote the model counterparts of the measurements, i.e., spectral densities or derived quantities; a_O^i are the measurements; and A_{ij} is a generally diagonal matrix. Therefore the first term represents the difference between model results and measurements. The vector $\bar{b}$ is a suitable set of parameters which describes the modification in the wind field; the magnitude of the second term with respect to the first one can be adjusted to allow a larger or smaller variation in the wind fields. The cost function must be minimized with the constraint of the model equations. The solution of the variational problem using the adjoint method has been proposed by *de Valk and Calkoen* [1989] for a regional implementation of the WAM model. *K. Hasselmann et al.* [1988] solved it with a different approach using Green's function, which describes the response of the wave field to small perturbations in the stress field.

The advantage of sequential methods is the relative simplicity and the relatively low requirement for computer resources. The minimization of the cost function typically requires a series of runs of the wave model. Consequently, the computer resources needed are larger than those needed to execute the model itself, while the resources that are requested by a sequential method are, in comparison, negligible. On the other hand, the variational approach avoids the problem of specifying correlation scales in model and observations, such scales being automatically produced by the model dynamics; moreover, as has been already anticipated, we sought a method that could work using only altimeter data, without the necessity of additional spectral information. The approach by Hasselmann et al. explicitly requires the availability of the measured spectra. In principle, this is not true for the adjoint method, although *de Valk and Calkoen* [1989] assumed the availability of SWH, mean period and mean direction in their numerical experiments. At present there is no evidence that a variational method performs better than a sequential one, but as research is rapidly progressing in this field, results are expected to be published within the next few years.

Therefore we decided to continue with a sequential approach, using the previous experience of two of the authors [*Janssen et al.*, 1989], that uses satellite altimeter data to analyze the wave spectra, following a research line common to the studies by *Esteva* [1988] and *Thomas* [1988]. The input information is therefore the SWH along the satellite track. The advantage of altimeter data is their abundance and reliability; the disadvantage is that the SWH is not a dynamical quantity in the wave models, but only an output information derived from the spectrum. This raises the problem of the reconstruction of the wave spectrum from the altimeter data. Consequently, the procedure is split into two steps: first the SWH data are used to construct an analyzed field of SWH by optimum interpolation (OI) (as described in the second section). The second step consists of the reconstruction of the spectrum from the analyzed SWH, i.e., applying a procedure to transform the first-guess spectrum into the analyzed one, using the information of its total energy only. Since in the WAM model the spectrum has a discrete representation with 300 degrees of freedom (12 direction and 25 frequency bins), its updating, using only the total energy, must involve some assumptions, which are discussed in the third section.

This study presents two realistic data assimilation experiments, which are carried out using the altimeter data supplied by Seasat and Geosat. A short data assimilation experiment is carried out using Seasat data, with the purpose of investigating in some detail the effect in the subsequent behavior of the model. Satellite data are assimilated for $1\frac{1}{2}$ days. A parallel run without assimilation is also carried out. The results of the two runs have been compared with the satellite data available in the forecast period following the end of the assimilation. The comparison describes the relevance and the duration of the effect of the assimilation. A longer experiment (with data assimilated for 10 days at the end of November 1988) has been carried out using Geosat data. During it, buoy data could be used as an independent data set to estimate eventual benefits by comparing them with the analyzed wave spectra that were produced by the assimilation.

The wave model used in this study is the WAM model [*WAMDI Group*, 1988] in a global implementation with a 3° grid step. This is a third-generation wave model which computes the wave spectrum $F(f, \theta, t, \bar{x})$, where the arguments are frequency f, direction θ, time t, and position $\bar{x}$. Both the parameterization of the spectral shape and of the source function $S(f, \theta, \bar{x}, F)$ are avoided by the explicit solution of the energy transport equation

$$\partial F/\partial t + \nabla(C_g F) = S \tag{4}$$

in the prognostic part of the spectrum. Here C_g is the wave group velocity and S is the source function representing the physical mechanisms that are involved in the evolution of the wave field [*WAMDI Group*, 1988]. As will become clear in the remaining part of the paper, the assimilation approach can be used for other models, although possibly some features (see section 3.2) might be particularly suitable for the WAM model.

2. Construction of an Analyzed Wave Height Field

No consolidated technique has been used in the past to spread the altimeter data on the model grid. *Janssen et al.* [1989] used the data only at the grid point where the measurement took place. *Esteva* [1988] actually attempted to spread the information preserving the local slope in the forecasted SWH field, but he abandoned this technique because results were unsatisfactory, preferring, like Janssen et al., to use the measured SWH only at the point of the measurement. *Francis and Stratton* [1990] used an exponential spreading function, estimating a correlation length of 1200 km from a collection of wave measurements in the North Sea. In this study, we use optimum interpolation, a standard procedure that has been extensively used in meteorology for data assimilation [*Hollingsworth*, 1986]. Here it is used to construct analysed significant wave height fields. At each point x_i the analyzed SWH, denoted as H_A^i, is expressed as a linear combination of $H_P^j (j = 1, \cdots, N_{\text{obs}})$, the first-guess results produced by the model, and of H_O^j, the observations:

$$H_A^i = H_P^i + \sigma_P^i \sum_{j=1}^{N_{\text{obs}}} W_{ij} \frac{H_O^j - H_P^j}{\sigma_P^j} \tag{5}$$

Here N_{obs} is the number of available observations and σ_P^j is the root-mean-square error in the model prediction,

$$\sigma_P^j = \langle (H_P^j - H_T^j)^2 \rangle^{1/2} \tag{6}$$

where H_T^j represents the true value of the SWH. The weights W_{ij} are chosen to minimize the root-mean-square error in the analysis, σ_A^i,

$$\sigma_A^j = \langle (H_A^j - H_T^j)^2 \rangle^{1/2} \tag{7}$$

The angle brackets indicate an average over a large number of realizations. Assuming that the errors in the model are uncorrelated with the errors in the measurements, the solution is

$$W_{ij} = \sum_{k=1}^{N_{\text{obs}}} P_{ik} M_{kj}^{-1} \tag{8}$$

where the element of the matrix M is

$$M_{kj} = P_{kj} + O_{kj} \tag{9}$$

and P and O are the error correlation matrices of prediction and observation, respectively (both are actually scaled with σ_P^i):

$$P_{kj} = \left\langle \frac{(H_P^k - H_T^k)(H_P^j - H_T^j)}{\sigma_P^k \sigma_P^j} \right\rangle \tag{10}$$

$$O_{kj} = \left\langle \frac{(H_O^k - H_T^k)(H_O^j - H_T^j)}{\sigma_P^k \sigma_P^j} \right\rangle \tag{11}$$

Therefore the prediction error correlation matrix P and the observation error correlation matrix O must be specified. This would require in practice the determination of statistics for both prediction and the observations, which are presently unavailable. Tentatively, for the prediction it is assumed

$$P_{kj} = \exp\left(-\frac{|\bar{x}_k - \bar{x}_j|}{L_{\max}}\right) \tag{12}$$

and the observation errors are assumed to be random and uncorrelated:

$$O_{ij} = \delta_{ij}(\sigma_O^i/\sigma_P^i) = \delta_{ij} R_i \tag{13}$$

The effect of variations of $L_{\max}$ and of the ratio between σ_O^i and σ_P^i on the results of the assimilation is discussed in the fourth section.

3. Analysis of the Wave Spectrum

Since only altimeter data are used in this study, the result of the OI is a SWH field. This of course specifies the total energy of the wave spectra but not their shape. Therefore in this kind of sequential method, some extra assumptions must be introduced to update the wave spectrum. *Esteva* [1988] simply multiplied the spectrum by the factor $(H_A/H_P)^2$ without modifying the wind speed. The problem of reconstructing the wave spectrum was further addressed by *Thomas* [1988], who attempted to reconstruct buoy spectra by combined measurements of significant wave height and wind speed using the JONSWAP spectrum [*Hasselmann et al.*, 1973]. The approach used here must be different, because a different type of wave model is involved. Both Thomas and Esteva used a second-generation wave model with a prescribed wind sea spectral shape, while in this study we use a third-generation wave model, where there is no prescribed spectral shape. Moreover, we prefer not to rely on the altimeter wind speed measurements and to use only wave data. An infinite number of transformations can be applied to the WAM model spectrum in order to match its energy with the measurements, and none of the produced spectra will introduce shocks in the model, although they may be actually very unrealistic and therefore not produce the expected improvement. Specifically, the multiplication of the swell spectrum by the factor $(H_A/H_P)^2$ does not produce satisfactory results in the WAM model [*Lionello and Janssen*, 1990].

The basic assumption of the reconstruction we propose is that the model prediction is wrong because the stress field by which it has been driven was incorrect. Consequently, we aim to obtain the spectrum that the model would have produced if the stress field were correct, consistently modifying also the wind speed. It is generally believed, at least among wave modelers, that most of the errors in the wave prediction are actually derived from errors in the stress field, and our assumption is in agreement with such an opinion.

The information contained in the first-guess spectrum $F_P(f, \theta)$ is used to produce an analyzed spectrum $F_A(f, \theta)$ as

$$F_A(f, \theta) = AF_P(Bf, \theta) \tag{14}$$

As no information on the direction of waves is provided by the altimeter, we are forced to consider only errors in the modulus of the stress and not in its direction, but if information on the direction were available, a third parameter could easily be introduced to rotate the spectrum. This solution is, of course, appropriate when no major feature of the true spectrum is absent in the first-guess spectrum; if a peak were completely missed, this approach would not be able to produce it. Moreover, the ratio among parts of the spectrum having a different origin cannot be changed. Therefore this approach cannot correct for large inaccuracies in the prediction, since this would imply a complete restructuring of the spectrum. We expect that it is adequate anyway for the operational framework for which it has been conceived, because both the analyzed wind fields driving the WAM model during the analysis and the regular repetition of the data assimilation process are expected to limit the discrepancies between model and observations. It must be stressed that (14) is not meant to describe the evolution of the wave spectrum, a task for which it is clearly inadequate, but to transform a first-guess spectrum into an analyzed one, which should have been generated in a relatively similar situation.

To determine the two parameters A and B in (14) is the purpose of the reconstruction procedure. The method distinguishes between the wind sea spectrum and the spectrum outside the storm region, reflecting the traditional distinction between wind sea and swell in wind wave modeling. The term "swell" in this study will be used in a relatively loose way to denote the situation in which the waves are not evolving under the effect of the wind. It is therefore applied also to the spectrum immediately outside the storm, which, in spite of being broad, cannot be considered wind sea because it has a peak frequency that is lower than the Pierson-Moskowitz frequency.

This section presents three simple situations to illustrate the reconstruction procedure. They are the reconstruction of the wind sea spectrum during time-limited growth (section 3.1), the reconstruction the spectrum during the subsequent decay when the wind drops (section 3.2), and the reconstruction of a spectrum in which wind sea and swell are present together owing to a sudden rotation of the wind (section 3.3). The idea is to compare three model runs: a first one, which will be referred to as correct prediction, is used to simulate the truth; a second one, obtained by introducing a bias in the surface stress, simulates the wrong prediction; and the third one, which will be referred to as the assimilation run simulates a run in which the assimilation is carried out. The assimilation run reproduces exactly the wrong prediction until the assimilation is carried out, extracting the measured value from the correct prediction and constructing the analyzed spectrum from the spectrum of the incorrect prediction. The assimilation produces an analyzed spectrum and, if the spectrum is wind sea, also an analyzed friction velocity. The assimilation experiment is successful if the assimilation run, which in its first part is identical to the wrong prediction, reproduces closely the correct prediction after the assimilation time. In these examples, since no OI is carried out, the measured SWH coincides with the analyzed one.

The model used is a single-point version of the WAM model in which advection is neglected, simulating an homogeneous ocean of infinite extent.

3.1. *Case A: Time-Limited Growth of Wind Sea*

The reconstruction of the wind sea spectrum is obtained using the energy growth curves and the relations between energy and mean frequency which describe its evolution. Note that these two equations are not explicitly present in the WAM model setup because the WAM model solves explicitly the energy transport equation, and they have to be derived by analytical fitting to the WAM model numerical results. The advantage of the wind sea, with respect to the swell, is that total energy and mean frequency can be made dimensionless to provide relations in a form that does not depend on the surface stress ρu_*^2 [*Kitaigorodskii*, 1962]. Dimensionless energy E_*, time t_*, and mean frequency f_{m*} are given as

$$E_* = \frac{u_*^4}{g^2} E \qquad t_* = \frac{g}{u_*} t \qquad f_{m*} = \frac{u_*}{g} f_m \tag{15}$$

where g is the acceleration of gravity and u_* is the friction velocity. We fit the WAM model numerical results and we obtained the following time-limited growth curve

$$E_*(t_*) = 955 \tanh (6.02 \times 10^{-5} t_*^{0.695}) \tag{16}$$

and the following relation between total energy and mean frequency during the wind sea development

$$E_*(f_{m*}) = 1.68 \times 10^{-4} f_{m*}^{-3.27} \tag{17}$$

(The mean frequency is here preferred to the peak frequency because its computation is more stable). The two curves are shown in Figures 1*a* and 1*b*).

These two relations are what we need to correct the effect of an error in the stress. In fact as the first-guess friction velocity that has been generating the waves is known, an estimate of the duration T of the wind sea can be derived using E_P in (16). Assuming that this estimate of the duration is correct, using the energy E_{*A} provided by the analysis in (16), an analyzed value of the friction velocity U_{*A} is computed. An analyzed value of the mean frequency f_{*mA} is derived using the computed U_{*A} and E_{*A} in (17). Finally, the dimensional quantities E_A and f_{mA} are provided by (15), and the two parameters A and B in (14) are given as

$$A = \frac{E_A}{E_P} B \qquad B = \frac{f_{mP}}{f_{mA}} \tag{18}$$

where E_P and f_{mP} are energy and mean frequency of the first-guess spectrum.

Figure 2 shows an instance of wind sea assimilation: in the incorrect prediction $u_* = 0.83$ and in the correct prediction $u_* = 0.64$. Figure 2a shows the time behavior of the SWH, Figure 2b shows that of the mean frequency, and Figure 2c shows that of u_*. After 12 hours the correct SWH is assimilated, obtaining, by the previously described procedure, an evaluation of the mean frequency and of the friction velocity. After the assimilation the evolution of the analyzed spectrum is very close to the correct prediction. This is a consequence of the correct analyzed friction velocity obtained by the analysis and of the correct reconstruction of the spectrum. This is shown in Figure 3 where correct, incorrect, and analyzed spectra are compared.

3.2. *Case B: Decay of the Spectrum in Absence of Wind*

As a second case the possibility to correct the spectrum during its decay is considered. The error is assumed to be due to the wrong friction velocity when the spectrum was generated, but the assimilation takes place when the wind has dropped and the spectrum is decaying. This is meant to simulate what happens on the border of a storm, where the dispersion has not yet spatially separated the different frequencies. The approach followed in case A is not possible because there is no way to produce dimensionless decay curves; the spectrum is then modified according to the method proposed by *Lionello and Janssen* [1990]. The authors investigated the decay of WAM model spectra which had been generated by different stresses. They found that, if the spectra have been decaying for the same time, the values of the average steepness s,

$$s = Ek_m^2/4\pi^2 \tag{19}$$

were very similar, in spite of very large differences in SWH and mean frequency. Therefore the authors suggested that the updating of the spectrum should not modify its steepness to construct the spectrum which should have been produced if the correct value of the friction velocity had been used during the generation. This produces for A and B the choices

$$A = \frac{E_A}{E_P} B \qquad B = \Delta B \left(\frac{E_A}{E_P}\right)^{1/4} \tag{20}$$

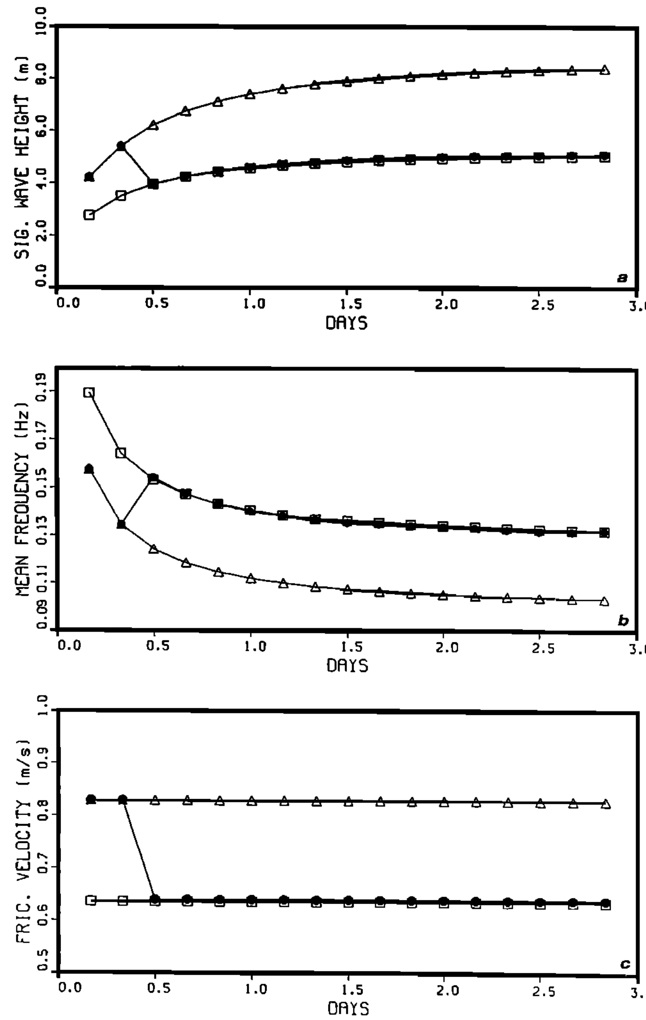

Fig. 2. Time series for case A (wind sea growth): (a) significant wave height, (b) mean frequency, and (c) friction velocity. Squares represent the correct prediction, triangles the incorrect prediction, and solid circles the assimilation run.

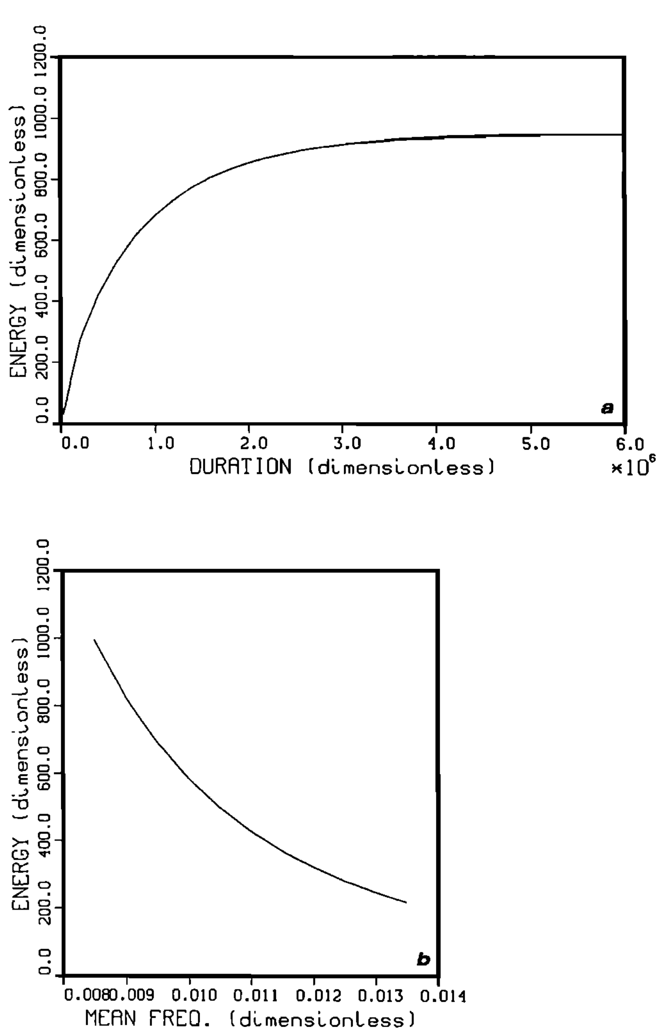

Fig. 1. Analytical fit to the WAM model results: (a) The dimensionless energy as function of the dimensionless time. (b) The dimensionless energy as function of the dimensionless mean frequency.

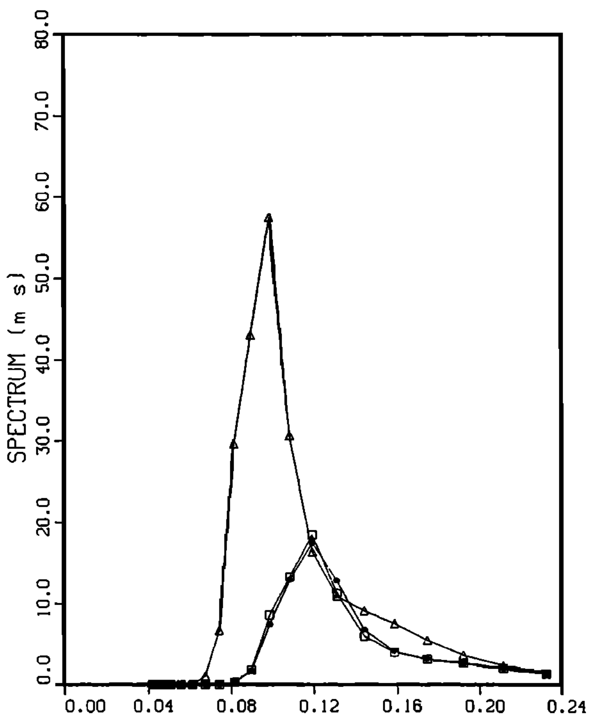

Fig. 3. Spectra at the assimilation time for case A. Squares represent the correct spectrum; triangles the first guess, i.e., the incorrect prediction; and solid circles the analyzed spectrum resulting from the assimilation.

where ΔB is a factor very close to 1 that can eventually be introduced to account for some variation in the steepness s observed in the model decay curves. This solution corresponds to the intuitive idea that a more energetic spectrum has a lower peak frequency; moreover, increasing the energy without decreasing the peak frequency would produce a swell with an unrealistic steepness and consequently a source function with an unrealistic dissipation [see *Lionello et al.*, 1991]. Since the swell spectrum is not related to the local stress, the analysis of the friction velocity cannot be carried out in this case, and the first guess value is not changed. Figure 4 shows the numerical experiment. The spectrum was generated by a wind that had been blowing for 2 days; in the correct prediction the friction velocity had a higher value, $u_* = 0.83$, than in the incorrect prediction where $u_* = 0.64$. After 1 day of decay the assimilation was carried out according to (20), resulting in the correct behavior of the model for the remaining part of the decay as shown in Figures 4*a* and 4*b*. The reason for the correct behavior is clear from the comparison of the spectra: Figure 5 shows the first-guess spectrum (squares), the correct spectrum (solid circles), and the result of the reconstruction (triangles). There is a very good correspondence between the reconstructed spectrum and the correct one. This implies a correct reconstruction also of the source function and therefore the reproduction of the correct decay, from the assimilation time onward.

3.3. *Case C: Spectrum Produced by a Sudden Change in Wind Direction*

Case C concerns a spectrum evolving under the action of a wind whose direction has changed, producing the simultaneous presence of wind sea and swell. The method presented in case A must be changed, because the evaluation of the duration from the total energy is clearly misleading and it will consequently produce an incorrect analyzed friction

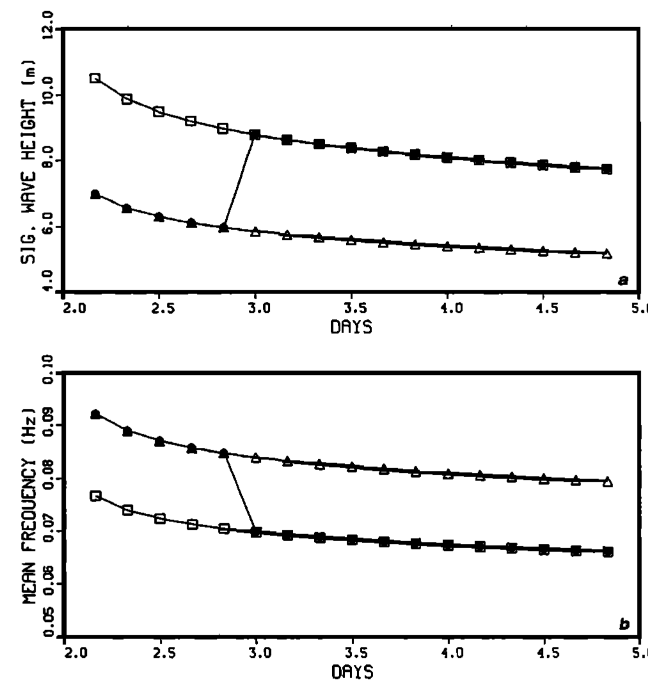

Fig. 4. Time series for case B (wave decay in absence of wind): (*a*) significant wave height and (*b*) mean frequency. Squares represent the correct prediction, triangles the incorrect prediction, and solid circles the assimilation run.

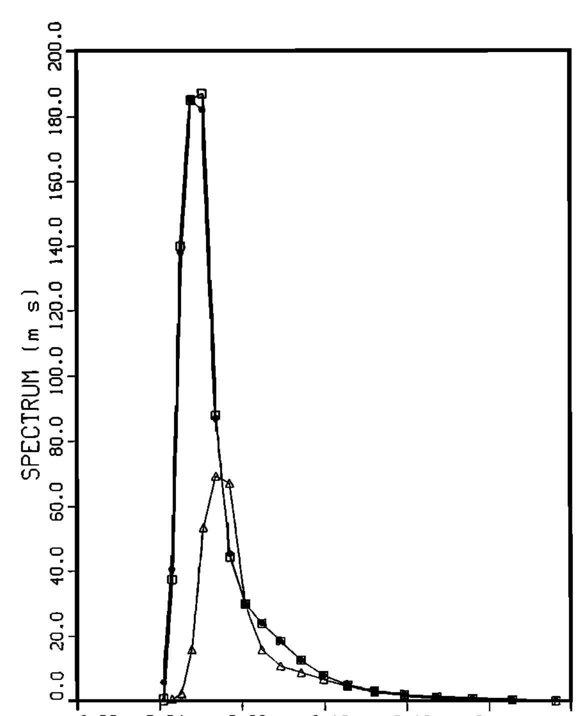

Fig. 5. Spectra at the assimilation time for case B (wave decay in absence of wind). Squares represent the correct spectrum; triangles the first guess, i.e., the incorrect prediction; and solid circles the analyzed spectrum resulting from the assimilation.

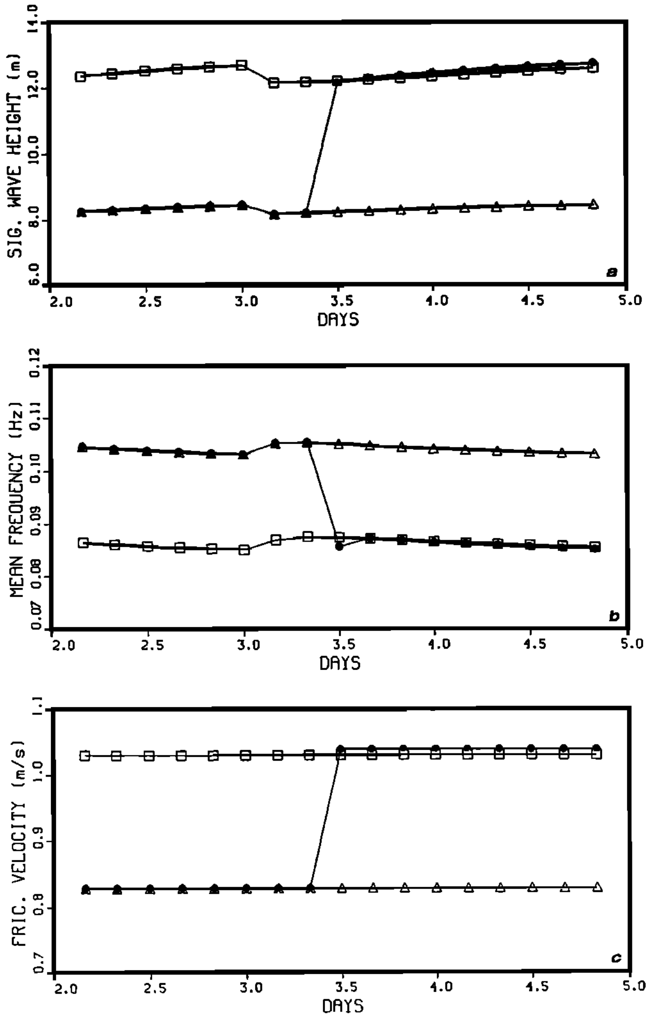

Fig. 6. Time series for case C (sudden change in the wind direction): (*a*) significant wave height, (*b*) mean frequency, and (*c*) friction velocity. Squares represent the correct prediction, triangles the incorrect prediction, and solid circles the assimilation run.

velocity. To produce a reasonable estimate, it is necessary to separate wind sea, which has been produced by the wind after the change in direction, from the remaining part of the spectrum; only the wind sea energy must be used to estimate the duration, which therefore approximates the period of time from the change of the wind direction. The first-guess wind sea energy $E_{P\mathrm{ws}}$ is estimated by locating the wind sea peak and computing the energy which has been generated by the wind in an area around it [see *Lionello et al.*, 1991]. The assimilation is then carried out as in case A, assuming that the ratio between wind sea energy and total energy is the same in the first-guess spectrum and in the correct one; the analyzed wind sea energy $E_{A\mathrm{ws}}$ is therefore given as

$$E_{A\mathrm{ws}} = \frac{E_A}{E_P} E_{P\mathrm{ws}} \tag{21}$$

The numerical experiment is along the same line as the previous ones: The wind blows for 3 days and then it changes its direction by 90°, without changing intensity. In the correct prediction $u_* = 0.83$ and the first guess has been produced by $u_* = 0.64$. The correct SWH is assimilated half a day after the change in the wind direction. Figure 6 shows how the prediction is corrected by the assimilation.

The effect of the assimilation on the two-dimensional spectrum can be evaluated in Figures 7*a*, 7*c*, and 7*d*, which show the first-guess spectrum, the analyzed spectrum, and the correct spectrum are shown respectively. There is a good correspondence between the analyzed and the correct spectrum. Figure 7*b* shows the part of the first-guess spectrum that has been considered wind sea.

3.4. *Considerations*

The reconstruction of the analyzed spectrum that is presented here works nicely in these simple cases, but it is expected of course to be less accurate in cases of complicated wind fields. In any case, when the separation of wind sea from the remaining part of the spectrum is relatively clear and the time-limited growth curve approximates the model behavior over a reasonable interval of time, the results of the wind sea assimilation using (14)–(18) are reliable. On the other hand, in realistic applications, the variability of the natural environment prevents obtaining the persistency of the benefits that is present in these synthetic cases.

Numerical experiments on decaying spectra [see *Lionello et al.*, 1991] show that the approach proposed in case B is consistent with the model dynamics over a region around the storm whose size is comparable to the size of the storm itself. This is because on such a scale, owing to the spatial extent of the storm, the spectrum contains a wide range of interacting frequencies and still has a quite active dissipation source function. Its extension to a distant region, where because of dispersion, the components of the spectrum separate in space, is debatable, but it may be supported by the loose argument that statistically, a higher SWH corresponds to a lower frequency. Anyway, if the assimilation is carried out in an operational framework, the continuous updating of the spectra in and around the generation area is expected to reduce the importance of the updating of the swell in a distant region unless systematic errors are present in the WAM model. The approach may produce inaccurate results when the interaction of the swell with newly generated wind seas or other systems affects the regular decay of the steepness, as observed in this experiment.

Discussing the result of experiment B, it is natural to ask if this approach has a general validity or it is applicable only to the WAM model. The answer can come only from the study of the decay of the spectrum immediately outside the generation area, where data are now lacking. It is obvious that if the behavior of the swell spectra in the WAM model is not realistic, the consequent systematic error will not be compensated by this assimilation scheme.

It must be noted, however, that the steepness of the spectrum is a quantity which must be dynamically relevant: the magnitude of the nonlinear source term S_{nl} is proportional to the square of the steepness

$$S_{\mathrm{nl}} \propto f s^2 F \tag{22}$$

The dissipation source function S_{ds} must moreover be in some way dependent on the steepness, according to the fact that steep waves are more likely to break than smooth ones. In the WAM model,

$$S_{\mathrm{ds}} = cf \left(\frac{f}{f_m}\right)^2 s^2 F. \tag{23}$$

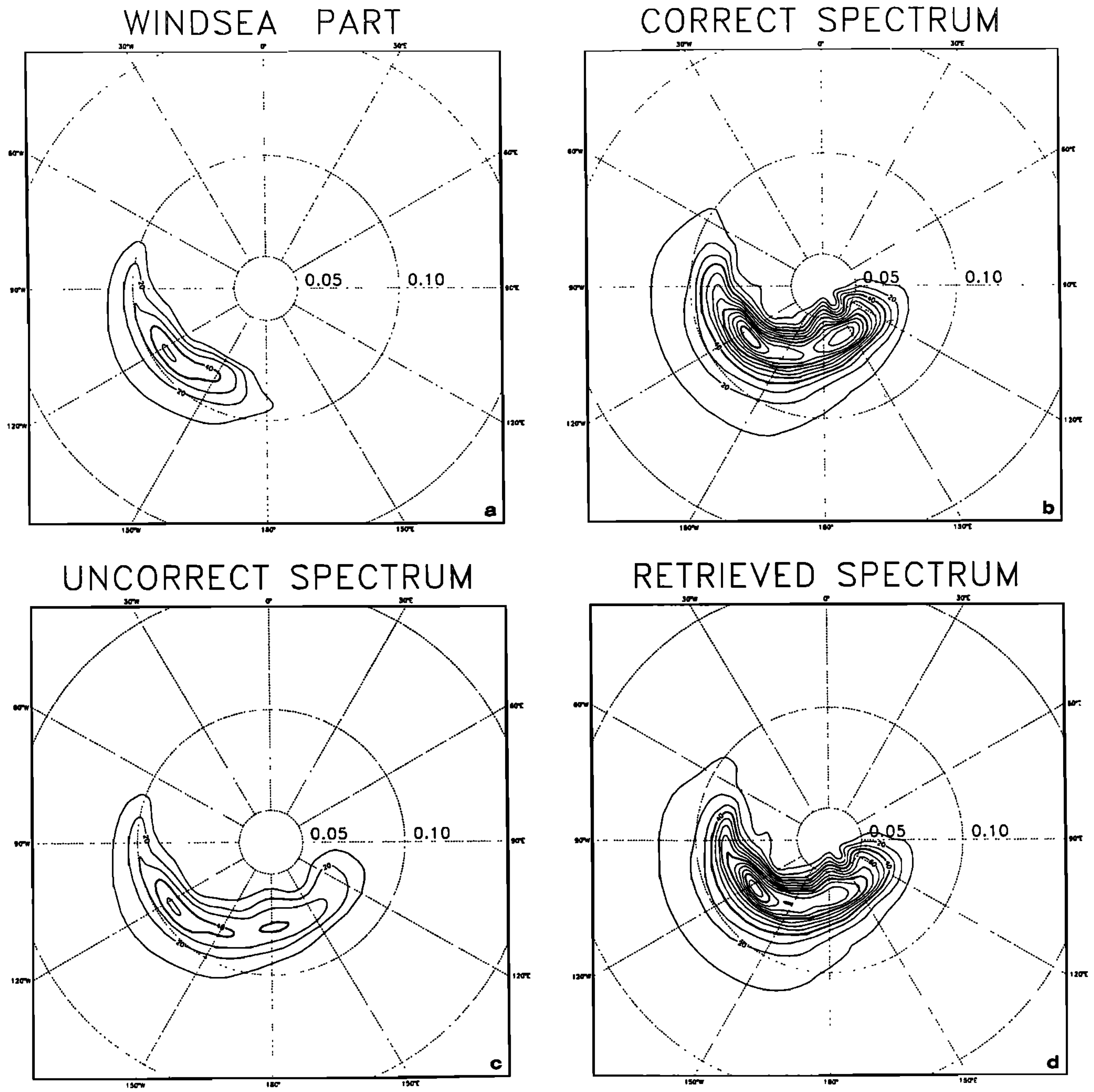

Fig. 7. Two-dimensional spectra at the assimilation time for case C: (*a*) first-guess spectrum from the incorrect prediction; (*b*) wind sea part of the first-guess spectrum, (*c*) analyzed spectrum, and (*d*) correct spectrum.

Therefore the quasi-conservation of the steepness by the assimilation implies that the source function strength is maintained inside a reasonable range, while an increment of the steepness increases the energy dissipation, producing a substantial reduction of the effect of the assimilation [*Lionello and Janssen*, 1990]. Although substantial inadequacies in the WAM model physics could make the results of this approach unrealistic, a simultaneous modification of energy and peak frequency is necessary to account for the different peak frequencies of swells which were generated by different wind speeds.

Finally, it is explicitly assumed that the errors in the wind field are mostly due to overevaluation or underevaluation, while direction and time behavior are substantially correct. This is a limitation of the method. In any case, corrections to the stress direction could be considered only if measurements of the wave directional distribution were available, and they could eventually be derived from an estimate of the spectral peak direction produced by SAR.

4. Effect of the Assimilation on the Forecast

This section investigates the effect of the assimilation of real satellite data in the WAM model results. The data that are used were produced by Seasat from the September 15, 1978, 12 UT, to the September 17, 1978, 12 UT. The period, the satellite data, and the wind fields (accurate global wind fields have been made available by *Anderson et al.* [1987]) are the same as in the study by *Janssen et al.* [1989].

A series of experiments were carried out. They have in common a first part, during which the model is spun up for 10 days from the September 5, 1978, 12 UT, to September 15, 1978, 12 UT (spin-up period); the field of spectra at the end of the spin-up period is used as initial condition for the assimilation experiments. The actual assimilation experiments begin at the end of the spin-up period, when the data contained in a time window of 12 hours (September 15, 12 UT to September 16, 0 UT) are assimilated in two different time steps, every 6 hours (analysis period). At each time step a field of analyzed SWH is produced by OI and is subsequently used to construct the wave spectra; the analyzed friction velocity that has been obtained is used to drive the wave model until a new stress field is provided by the atmospheric model (i.e., for the following 3 hours in the present setup of the WAM model). In the following $1\frac{1}{2}$ days (forecast period) the model is compared with the remaining satellite data that, not having been used in the assimilation, can be used to estimate the impact and the benefit of the assimilation; the degree of agreement between model and observations during the forecast period provides an estimate of the effectiveness of the assimilation. The comparison with a reference run, in which no assimilation has been carried out, makes it possible to study the decay of the effect of the assimilation. The length of the assimilation period has been limited to half a day, in order to analyze the spectrum only once in most of the grid points while providing coverage that is good enough to analyze waves over most of the ocean.

This short experiment, in which the actual length of the model run is only 2 days, can be performed quite inexpensively, making it possible to produce a series of experiments and to obtain an evaluation of the effect of variations in the correlation length $L_{\max}$, and in the root mean square error of the observations σ_O^i. As the method distinguishes between windsea and swell, the eventually different impact of the two distinct contributions and, correspondingly, of the use of (18) or (20) to the assimilation are examined. Our discussion begins considering the dependence of the results on $L_{\max}$. To this purpose, we computed the statistics of the model results against the altimeter measurements. Specifically we discuss here the effect on bias and root mean square error rms given by

$$\text{bias} = \frac{1}{N_{\text{obs}}} \sum_{j=1}^{N_{\text{obs}}} H_P^j - H_O^j \tag{24}$$

$$\text{rms} = \left[\frac{1}{N_{\text{obs}}} \sum_{j=1}^{N_{\text{obs}}} (H_P^j - H_O^j)^2 \right]^{1/2}$$

Figures 8*a* and 8*b* show the bias and the standard deviation, respectively, for the whole forecast period as functions of $L_{\max}$, which is expressed in grid units (the grid step is 3°). All the assimilation experiments significantly improve with respect to the reference run (whose bias and rms are represented by the solid line in both the figures). The benefits grow as $L_{\max}$ grows; the differences are relevant for low values of $L_{\max}$, but they saturate to a value showing very little dependence on it as $L_{\max}$ increases. In our opinion this

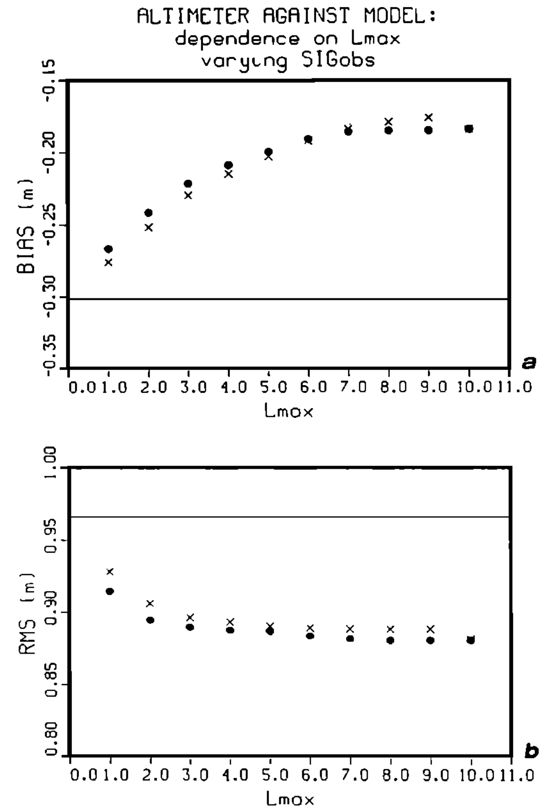

Fig. 8. Statistics of model results against altimeter observations for the whole forecast period: (*a*) bias and (*b*) standard deviation. The reference run is represented by the solid line; solid circles represent experiments with $R = 0.0$, where $R = \sigma_O/\sigma_P$, and crosses represent experiments with $R = 1.0$.

is the consequence of the separation between adjacent satellite tracks (which is roughly seven or eight grid points). Since in half a day the satellite completes almost seven orbits, almost any grid point is updated when $L_{\max}$ is larger than 4. A further increase affects the use of the satellite measurements because it compensates interruptions in the series along the tracks, and locally it changes the analyzed SWH because more observations contribute to the interpolation, but the resulting values are not substantially modified.

To investigate how the benefits of the assimilation persist in time, the statistics against measurements have been computed every 6 hours during the forecast period. Results are shown in Figure 9 for various choices of $L_{\max}$. The reduction of the absolute value of the bias with respect to the reference run persists for a long time, a reduction of 25% still being present $1\frac{1}{2}$ days after the end of the assimilation. The reduction of the standard deviation is less prolonged but it is still about 10% 1 day after the end of the assimilation.

These numerical results indicate that the correlation length $L_{\max}$ is larger than 5. This is actually an average over different situations. In fact, wind sea has a spatial correlation similar to the spatial extent of the generating storm, which is generally smaller than the spatial correlation of swell.

The results shown in Figure 8 already indicate that there is not a sensitive dependence on the value of the ratio $R = \sigma_O/\sigma_P$, and in fact differences cannot be considered statistically significant. Figure 10 shows the time behavior of the

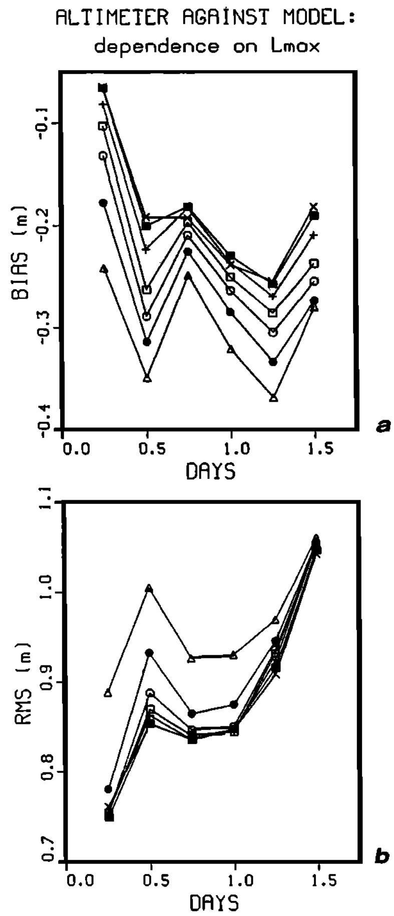

Fig. 9. Statistics of model results against altimeter observations computed every 6 hours during the forecast period: (*a*) bias and (*b*) standard deviation. Triangles represent the reference run; solid circles, $L_{max} = 1$; open circles, $L_{max} = 2$; open squares, $L_{max} = 3$; pluses, $L_{max} = 5$; solid squares, $L_{max} = 7$; and crosses, $L_{max} = 9$.

statistics for $L_{max} = 5$ for $R = 0, 0.5, 1, 2$. The choice $R = 2$ produces the worst results, while $R = 0$ and $R = 1$ produce quite similar results. This indicates that the errors in the altimeter are comparable to or smaller than the errors in the WAM model.

We now briefly examine the impact of the assimilation, considering the case with $L_{max} = 5$ and $R = 0$. Figure 11 shows the differences between assimilation and reference at the end of the assimilation period, on September 16 at 0 UT: isolines are plotted every 0.5 m and dots denote areas where the assimilation has reduced the SWH with respect to the reference. Most of the effect of the assimilation is of course in the southern hemisphere, on the track of the major storms. The general tendency of the model is to overevaluate with respect to measurements, with the exception of a storm in the Pacific, where the SWH is underevaluated. Since the overevaluation can be clearly distinguished inside the generation areas, it is related to an overevaluation of the wind speed (see Figure 12). Consequently the swell is generally overevaluated as well. It must be stressed that this is an unlikely situation for obtaining large benefits by the assimilation, because, as soon as the assimilation terminates, the action of the wind again produces wave growth, making the decrease of energy not very effective. The opposite case, in which the energy of a wave system is increased by the analysis, offers more evident benefits because at the end of the assimilation, the analyzed waves propagate over a field of less energetic waves, losing little energy and determining a persistent feature in the SWH pattern. Figure 13 shows what is left of the differences 1 day after the end of the assimilation. The pattern is of course much smoother than that in Figure 11, but differences up to 1 m are still present in the southern ocean. The individual features tend to move eastward because of the predominant direction of the waves generated by storms in the southern hemisphere. Two updated swell systems that have been radiated from the midlatitudes toward the equator are present around 170°W, 10°S, and 130°W, 18°S. Their origin can be traced back in Figure 11 to 162°W, 18°S, and 129°W, 15°S, respectively.

To investigate whether wind sea or swell updating is more effective, two experiments were performed analyzing only wind sea or swell spectra. In the first case, the assimilation was carried out only in the points where (according to the model) most of the spectrum is wind sea and using (18); in the second case, only points where most of the spectrum is swell were updated using (20). Of course, the wind sea is relatively localized on the global scale, and this consideration would suggest that the updating of swell could have a much larger impact. Moreover, the swell should have a longer memory. Although supporting these arguments our

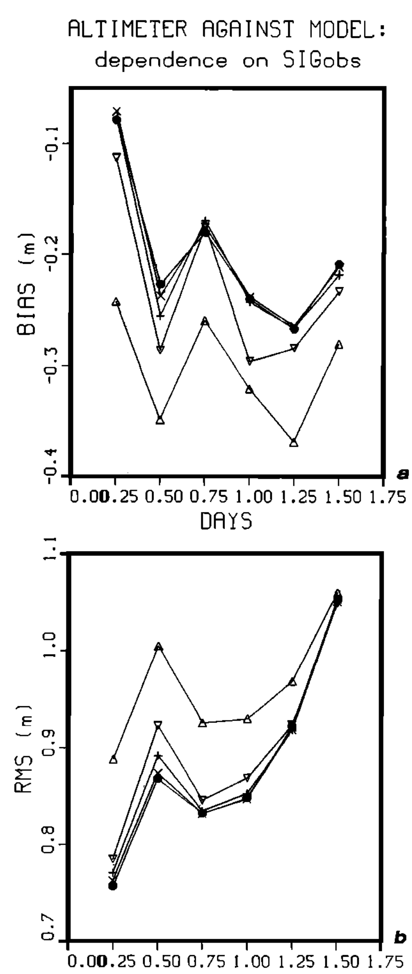

Fig. 10. Statistics of model results against altimeter observations computed every 6 hours during the forecast period: (*a*) bias and (*b*) standard deviation. In all experiments, $L_{max} = 5$. Triangles represent the reference run; solid circles, $R = 0$; crosses, $R = 0.5$; pluses, $R = 1$; and nablas, $R = 2$.

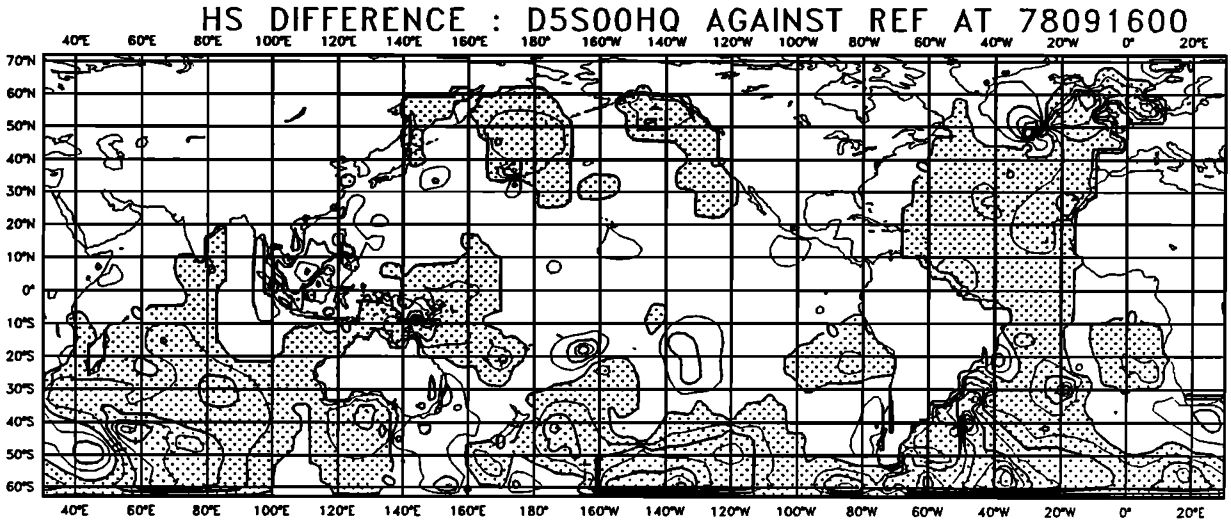

Fig. 11. Differences between assimilation run (R = 0, L_{max} = 5) and the reference run at the end of the assimilation period. The quantity plotted is $H_A - H_R$. Isolines are drawn every 0.5 m; dotted areas indicate negative values.

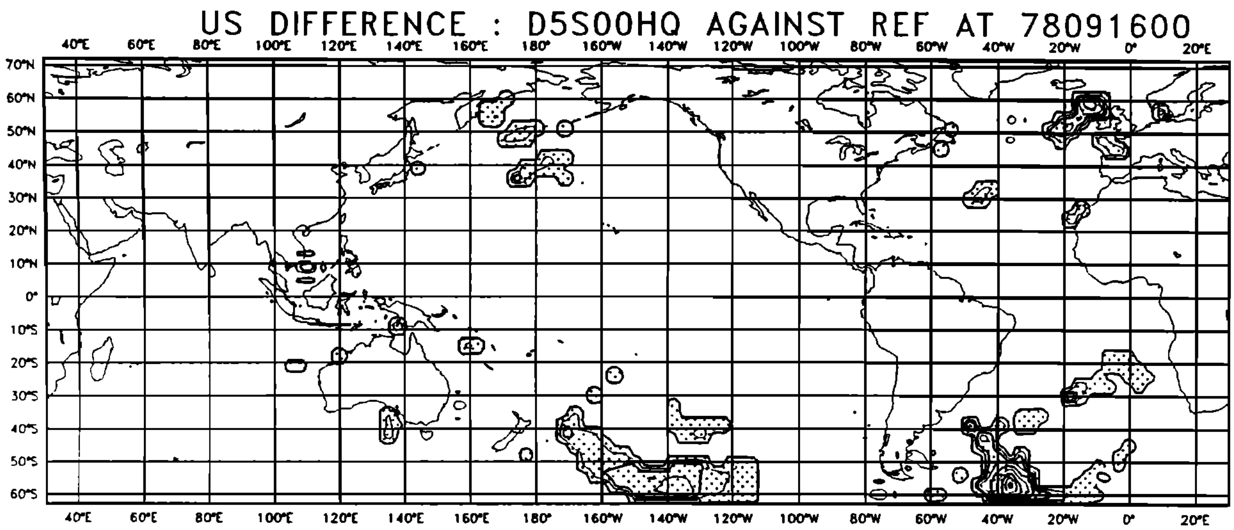

Fig. 12. Differences between assimilation run (R = 0, L_{max} = 5) and the reference run at the end of the assimilation period. The quantity plotted is $u_{*A} - u_{*R}$. Isolines are drawn every 0.05 m/s; dotted areas indicate negative values.

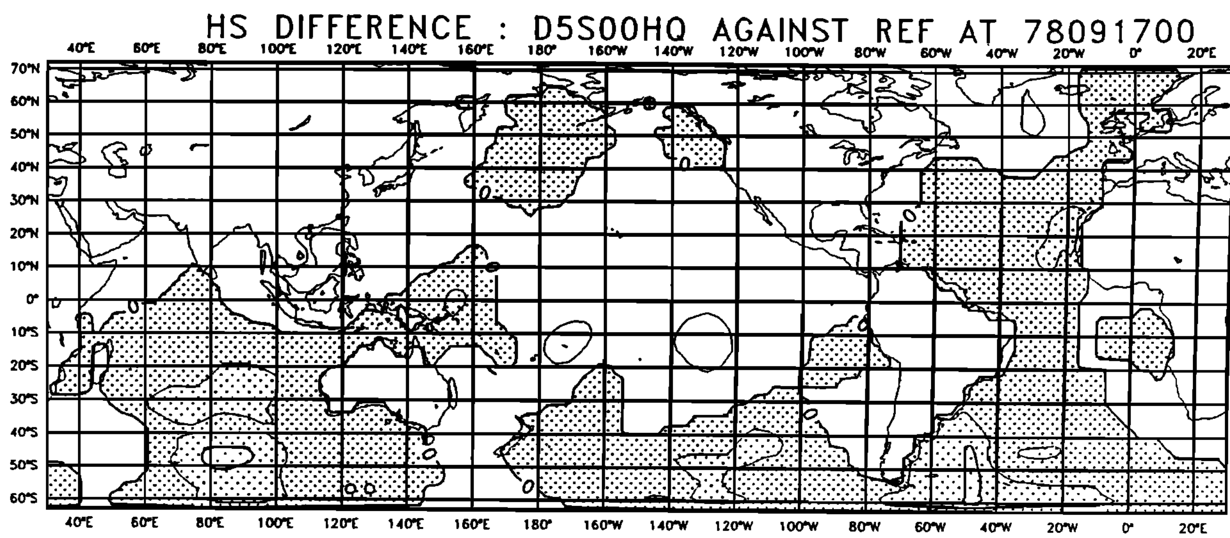

Fig. 13. Differences between assimilation run (R = 0, L_{max} = 5) and the reference run 1 day after the end of the assimilation period. The quantity plotted is $H_A - H_R$. Isolines are drawn every 0.5 m; dotted areas indicate negative values.

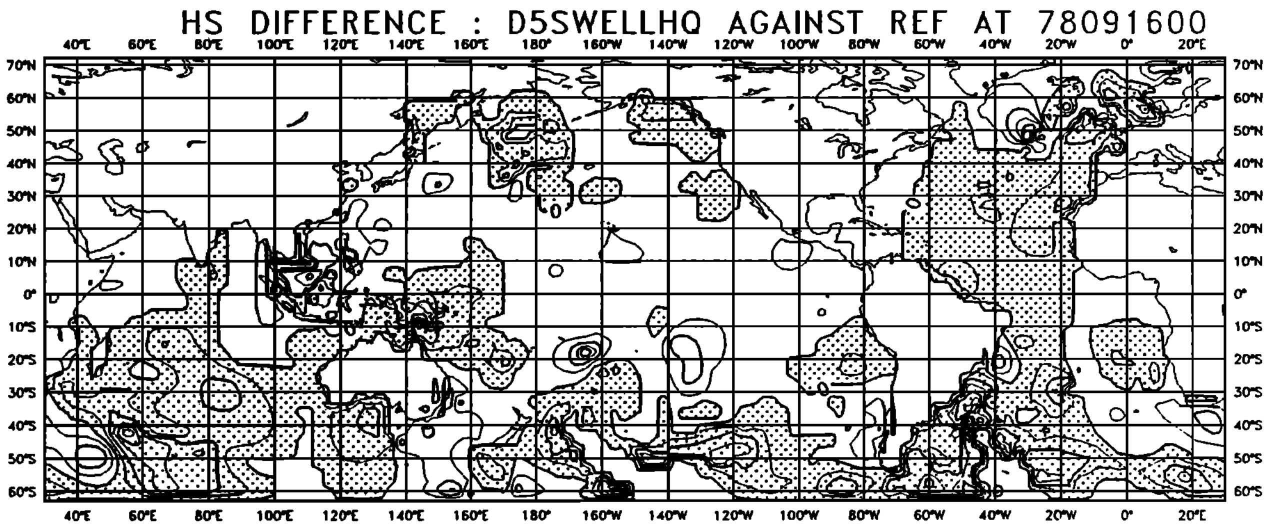

Fig. 14. Differences between swell assimilation run ($R = 0$, $L_{max} = 5$) and the reference run at the end of the assimilation period. The quantity plotted is $H_A - H_R$. Isolines are drawn every 0.5 m; dotted areas indicate negative values.

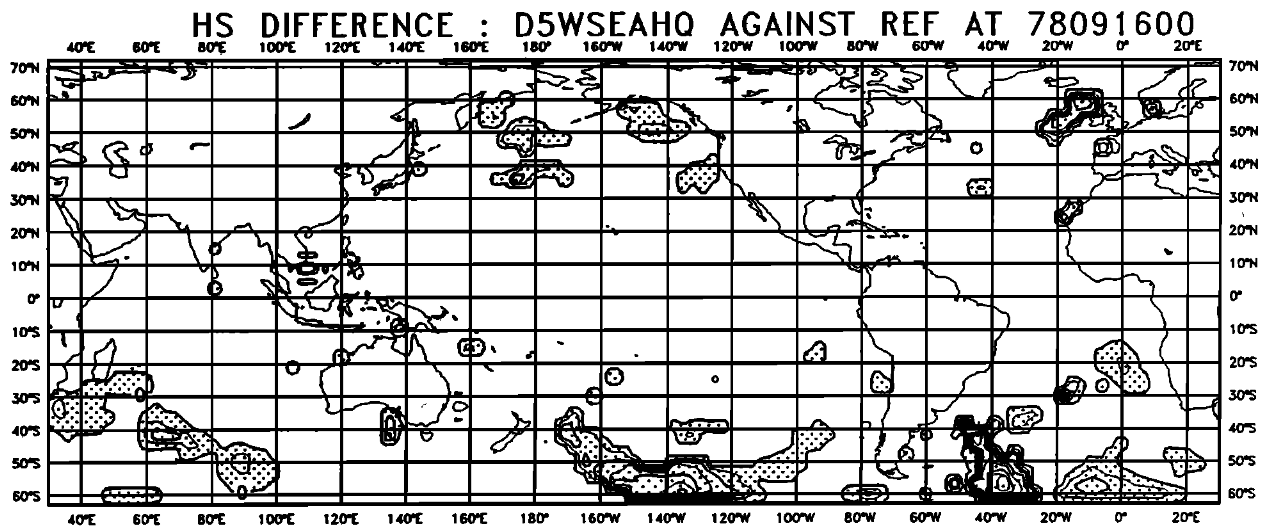

Fig. 15. Differences between wind sea assimilation run ($R = 0$, $L_{max} = 5$) and the reference run at the end of the assimilation period. The quantity plotted is $H_A - H_R$. Isolines are drawn every 0.5 m; dotted areas indicate negative values.

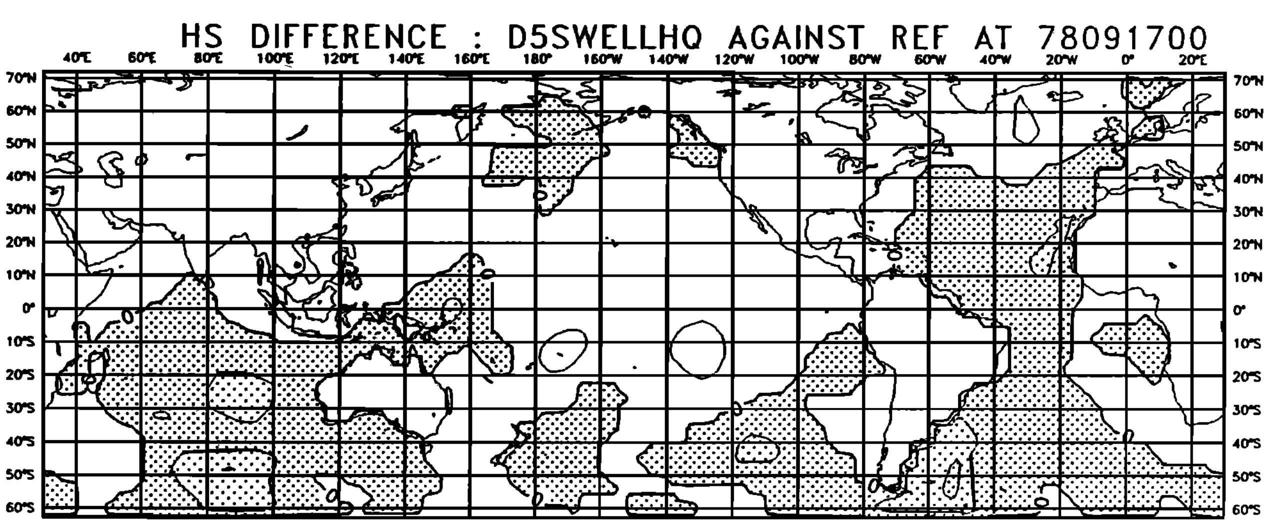

Fig. 16. Differences between swell assimilation run ($R = 0$, $L_{max} = 5$) and the reference run 1 day after the end of the assimilation period. The quantity plotted is $H_A - H_R$. Isolines are drawn every 0.5 m; dotted areas indicate negative values.

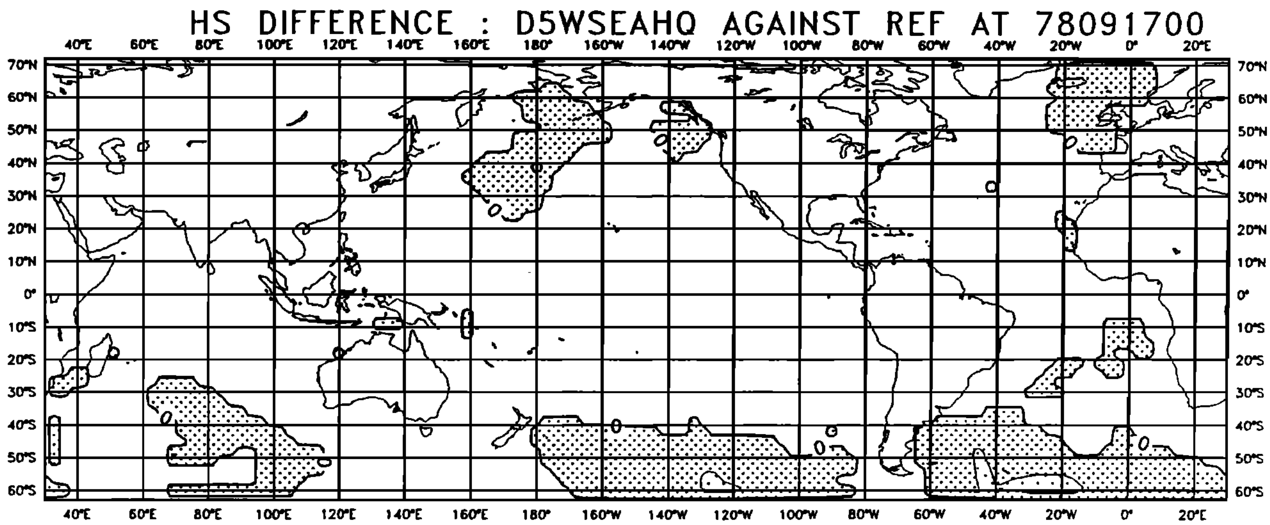

Fig. 17. Differences between wind sea assimilation run (R = 0, L_{max} = 5) and the reference run 1 day after the end of the assimilation period. The quantity plotted is $H_A - H_R$. Isolines are drawn every 0.5 m; dotted areas indicate negative values.

experiments indicate that the impact of wind sea updating is quite comparable to the impact of swell updating. Figures 14 and 15 show the difference that has been introduced by assimilating swell and wind sea, respectively, with respect to the assimilation run. The swell assimilation determines a much more widespread pattern, while the effect of the wind sea assimilation is localized in the southern ocean but is very important in this region. One day after the end of the assimilation, the difference introduced by swell assimilation is slightly larger than that introduced by wind sea assimilation (see Figures 16 and 17), but because of the large differences introduced by wind sea assimilation in the southern part of the globe, the impact of the two experiments is quite comparable.

The statistics support the same conclusions. Global statistics (Figure 18) indicates that updating of wind sea and swell have the same importance for the successive forecast. In fact, they are important in different regions. Figure 19 shows the statistics limited to an region around the equator (i.e., for latitudes between 15°N and 15°S) where the effect of the swell dominates, being responsible for almost the whole improvement obtained by the assimilation. This is of course because the sea state around the equator is mostly swell radiated by mid-latitude storms. If the statistics are restricted to the southern part of the globe (i.e., latitudes south of 15°S), then the effect of wind sea analysis is more important because of the many storms present inside which the waves were overevaluated (see Figure 20). These results indicate that a data assimilation approach should not be limited to the analysis of the wind sea, but methods should also analyze swell to be successful on a global scale.

5. VERIFICATION OF THE ANALYSIS AGAINST BUOY OBSERVATIONS

In this section we compare the results of the analysis, performed using altimeter data, with buoy measurements, which are not used in the assimilation. Data are provided by NOAA buoys, that have actually already been used to verify the model results [*Zambresky*, 1988]. In order to obtain an extensive set of data for the comparison, the assimilation of

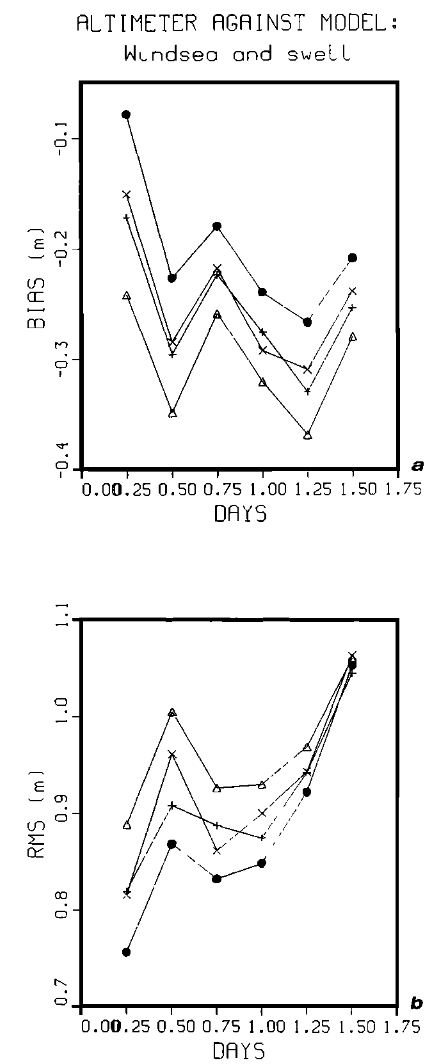

Fig. 18. Global statistics of model results against altimeter observations computed every 6 hours during the forecast period (L_{max} = 5; R = 0): (a) bias and (b) standard deviation. Triangles represent the reference run; crosses, swell assimilation only; pluses, wind sea assimilation only; and solid circles, complete assimilation.

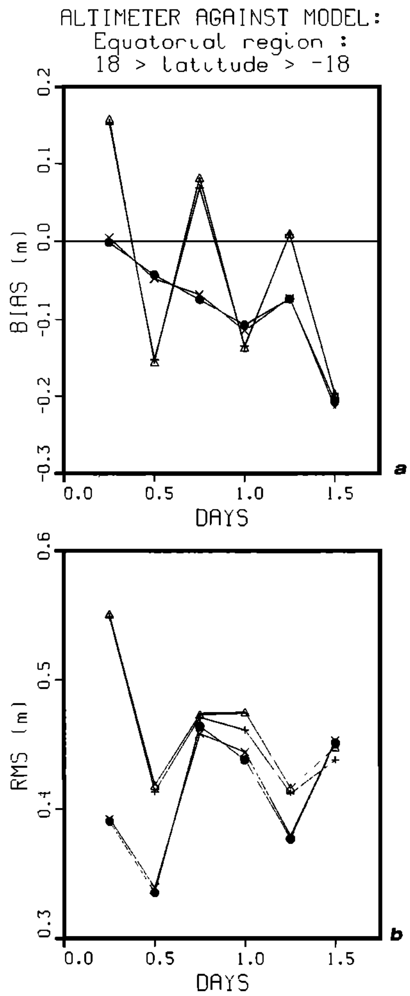

Fig. 19. Statistics of model results against altimeter observations computed every 6 hours during the forecast period for the equatorial region (L_{max} = 5; R = 0): (*a*) bias and (*b*) standard deviation. Triangles represent the reference run; crosses, swell assimilation only; pluses, wind sea assimilation only; and solid circles, complete assimilation.

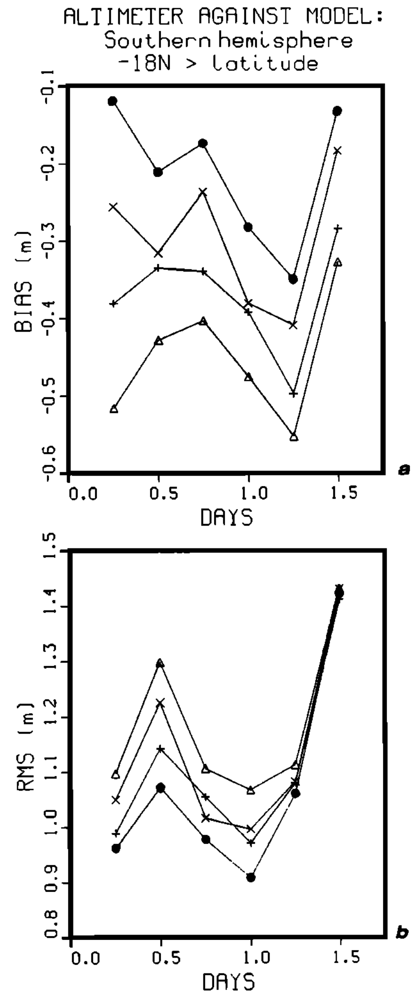

Fig. 20. Statistics of model results against altimeter observations computed every 6 hours during the forecast period for the southern part of the oceans: (*a*) bias and (*b*) standard deviation. Triangles represent the reference run; crosses, swell assimilation only; pluses, wind sea assimilation only; and solid circles, complete assimilation.

wave observations was carried out every 6 hours in the last 10 days of November 1988 (from November 20, 18 UT, to November 30, 24 UT). During this period the WAM model was driven by the analyzed wind fields produced by the European Centre for Medium Range Weather Forecasts (ECMWF) atmospheric circulation model. Four experiments were carried out choosing different combinations of the parameters in the OI: L_{max} = 3 and R = 0, L_{max} = 3 and R = 1, L_{max} = 5 and R = 0, and L_{max} = 5 and R = 1. The analyzed wave data were provided by the altimeter mounted on Geosat. A parallel reference run, without any assimilation, was carried out for comparison. The discussion involves of course some inspection of specific cases to identify the reasons of the success or failure of the assimilation. Two relevant and representative situations are discussed, considering buoy measurements at Hawaii and in the Gulf of Alaska.

The area around Hawaii is an interesting location because the swell that is radiated by the storms in the northern hemisphere can be detected. Figure 21 shows the time series of NOAA buoy 51002, located at 17.2°N, 157.8°W, and of the model runs for the four previously mentioned cases. The arrows indicate the time when the spectra are compared in Figure 22. The buoy significant wave height is produced every hour, but measurements are averaged over a 6-hour time window for a more adequate comparison with model results, which are produced with a 6-hour output step. In Figure 22, buoy measurements are denoted with crosses, the results of the reference run with triangles and of the assimilation experiment with solid circles. The nearest grid point of the model is taken for the comparison. The impact of the assimilation is clearly positive: a series of relevant wave systems, missing in the reference run but present in the buoy record, have been detected by the satellite. The improvements corresponding to the satellite passages can be clearly distinguished in the time series in Figure 21.

The differences between the choices L_{max} = 3 and L_{max} = 5 are caused by use of more distant satellite tracks in the latter case, allowing the spectrum to be updated a larger number of times at the buoy location. The better results have been obtained with L_{max} = 5, indicating a large spatial correlation in the wave field, probably associated with a massive presence of swell. This confirms the trend in the dependence of the results on L_{max} that was found in the

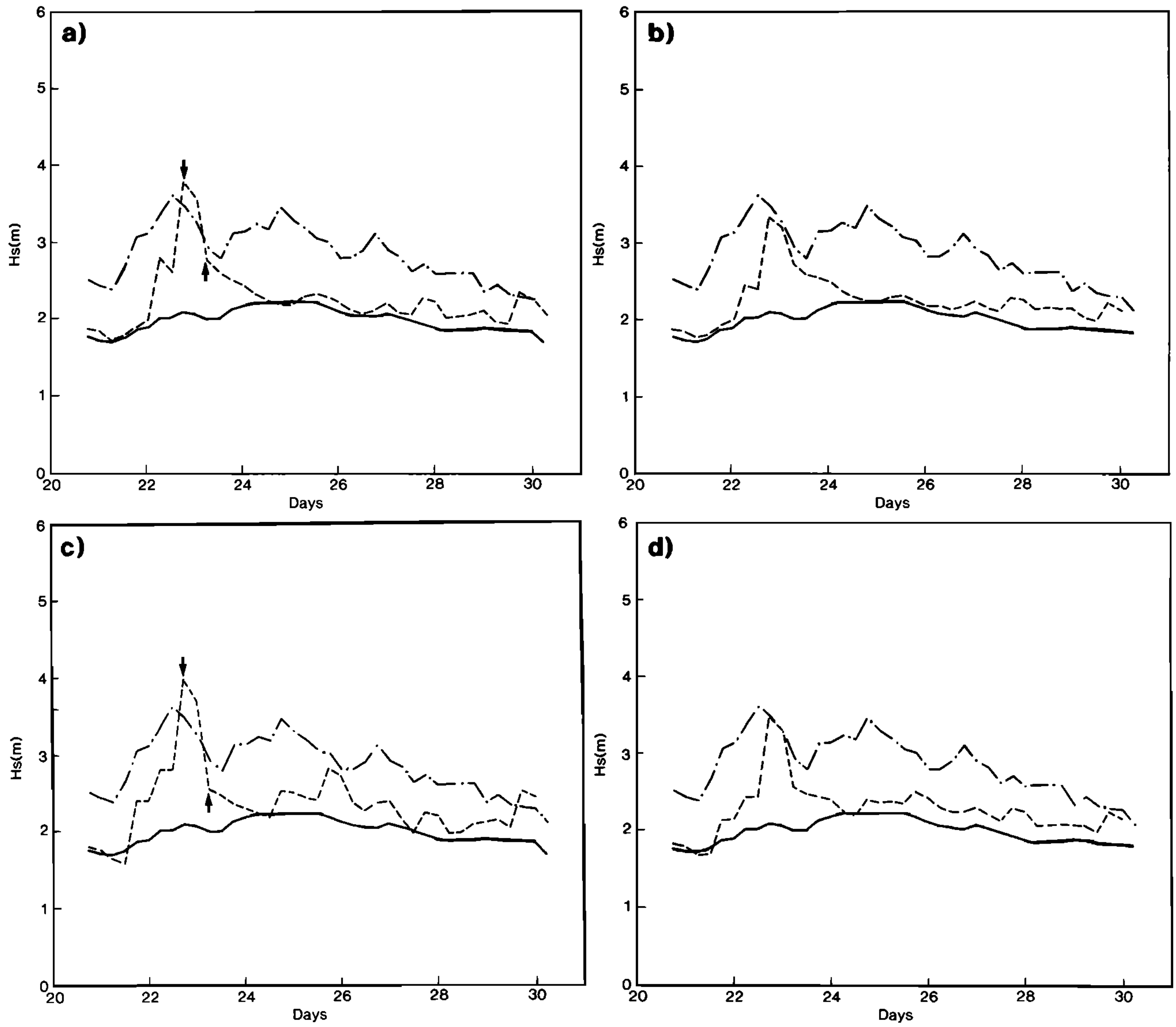

Fig. 21. SWH time series at buoy 51002. Dash-dot lines indicate buoy measurements; solid lines, reference experiment; and dashed lines, assimilation experiments. Each figure shows a different data assimilation experiment: (*a*) $L_{max} = 3$, $R = 0$; (*b*) $L_{max} = 3$, $R = 1$; (*c*) $L_{max} = 5$, $R = 0$; and (*d*) $L_{max} = 5$, $R = 1$.

previous section (see Figure 8). The magnitude of the corrections depends on R and is of course larger for $R = 0$. In this case, this is always the best choice. Table 1 reports the time series statistics which shows how the assimilation improves the model results with respect to the reference run, the best results having been obtained using $L_{max} = 5$, $R = 0$. Note that the effect of the assimilation is irrelevant for some periods; this is because of the presence of unreliable spikes in the data close to the buoy location, which prevented the use of data in part of the satellite tracks.

Figure 22 shows the one-dimensional buoy spectra and the model spectra in correspondence to two relevant cases, producing an example of the improvement obtained as a result of the assimilation.

Figures 23 and 24 aim to show the situation at the time of the previously compared spectra. The upper large figure shows the wave field in the reference run, and the lower one shows the difference introduced by the assimilation. In both figures the line shows the satellite track. The measurements along the satellite track are reported in the upper right figure, which also displays the time of the satellite passage. The assimilation on November 22 at 18 UT, corresponding to the spectra in Figure 22*a*, corrects a substantial underevaluation of the SWH in the reference run in a area south of Hawaii (Figure 23). In the second case, on November 23 at 6 UT the effect is smaller because the error in the reference run was smaller (Figure 24). Although it is tempting to claim a satisfactory success in this case, examining the results of the assimilation at Hawaii, it must be realized that this is a case of a complicated spectrum (many wave systems are present at the same time) for which the reconstruction of the spectrum is not expected to be accurate. In fact, wind sea and swell are both modified, while they are not necessarily both wrong.

The results in the Gulf of Alaska are less satisfactory. In fact, at buoy 46002, at 42.5°N, 130.4°W, the impact is less relevant than at Hawaii, and it does not always improve the results (Figures 25 and 26). Although in correspondence to

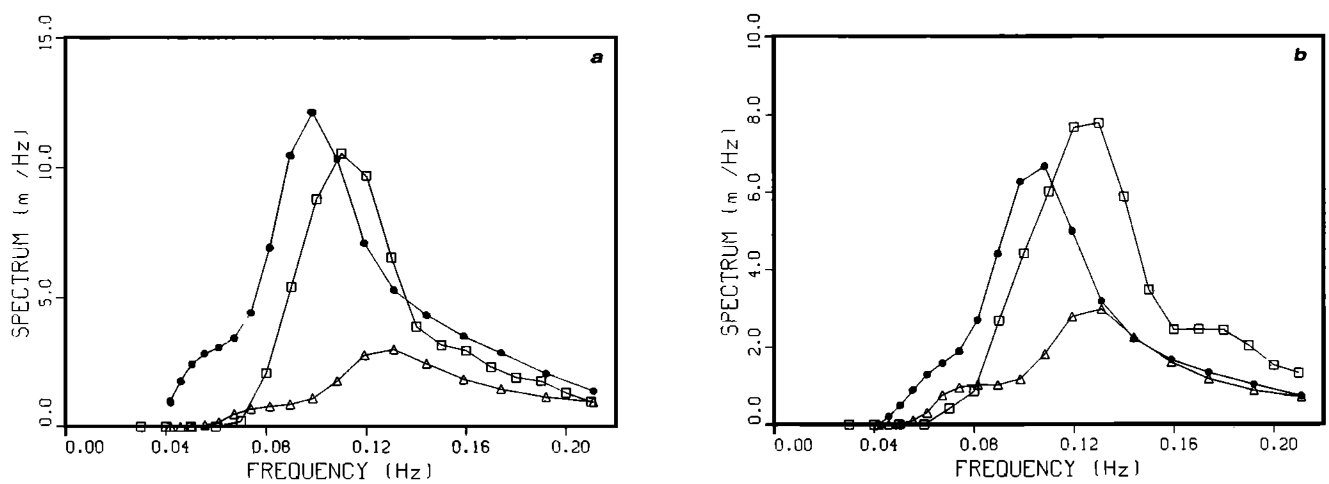

Fig. 22. Spectra at buoy 51002 for (*a*) November 22, 18 UT, and (*b*) November 23, 6 UT. Squares represent the buoy spectrum; triangles, the reference spectrum, and solid circles, the analyzed spectrum (L_{max} = 3; R = 0).

the major event, taking place from November 22 to November 25, the modification has the correct tendency, it is too small to substantially improve the agreement of model and observations. On the other hand, during the second relevant event, which took place from November 28 to November 29, the assimilation acts in the wrong direction, increasing the negative bias instead of reducing it (see Figure 25). In the statistics, shown in Table 1, the two modifications compensate each other, producing very little change in the resulting values. We investigated two specific cases to get a picture of the situation.

Consider the situation on November 23 at 6 UT, which is shown in Figure 27. The time series shows that at that time and in the following 24 hours the reference run produced a SWH 2 m less than the buoy measurement and the assimilation could not compensate it, producing an improvement of less than 1 m. The assimilated data were extracted from the satellite passage shown in Figure 27, which is substantially in agreement with the reference run. Changes in the SWH field were produced more by the symmetric spread of the information across the satellite track than by the measured values themselves. There may be two explanations for the failure of the assimilation: there is an inconsistency between altimeter and buoy measurements (the altimeter being biased low with respect to the buoy), or the real wave field has a strong gradient, which is completely missed by the WAM results, possibly as a result of local conditions at the buoy location. Both factors may eventually contribute.

TABLE 1. Statistics of the Various Numerical Experiments Against the Data of Buoy 51002, Located at Hawaii, and of Buoy 46002 in the Gulf of Alaska

Run	Bias	Standard Deviation
	Buoy 51002	
R = 0, L_{max} = 3	0.60	0.71
R = 1, L_{max} = 3	0.63	0.71
R = 0, L_{max} = 5	0.52	0.63
R = 1, L_{max} = 5	0.59	0.67
Reference	0.87	0.91
	Buoy 46002	
R = 0, L_{max} = 3	0.95	1.17
R = 1, L_{max} = 3	0.93	1.14
R = 0, L_{max} = 5	1.02	1.23
R = 1, L_{max} = 5	0.96	1.16
Reference	0.92	1.22

A successive satellite passage is closer to the buoy than the previous one (see Figure 28). The reference run in this case produced values 1.5 m less than the buoy measurements. Again the assimilation can compensate only partially for this discrepancy. This case reinforces the hypothesis that the altimeter is biased low with respect to the buoy. Actually, the instrument specification indicates an error of 10% or 0.5 m, whichever is larger, which in this case is of the order of the lacking SWH, but this is not meant to be related to the systematic bias that we may be observing in these cases.

Therefore the data assimilation could not recover the correct value because the extreme waves recorded by the buoys were less energetic in the altimeter measurements. There are indications that this is because of a systematic bias of satellite altimeter and buoy measurements. At Hawaii, where waves were smaller, the problem was not evident; it may be limited only to extreme cases. The other possibility is that local details have been missed by the satellite passages, and the spread of the information that was obtained by OI smoothed them, producing a fake reconstruction of the wave field. Of course the problems may both be present.

Zambresky [1988] already suggested that the WAM model was producing an excessive energy decay on the border of the storms. Examining the results of these experiments, we have the same feeling. In fact, at Hawaii a relevant part of the spectrum was presumably swell, and also for the cases in the Gulf of Alaska it is sensible to expect a relevant contribution from waves produced by a distant storm or evolving on the border of the stormy region. In both the cases the WAM model underpredicted with respect not only to buoys but also to the altimeter. This is relatively surprising because it was shown in section 4 that in the storms SWH was overevaluated and the same conclusion holds in most of the cases also for this experiment. It appears therefore that the energy decay on the border of a storm is excessive in the WAM model, not only compensating the previous overprediction but even determining an underprediction of the wave energy.

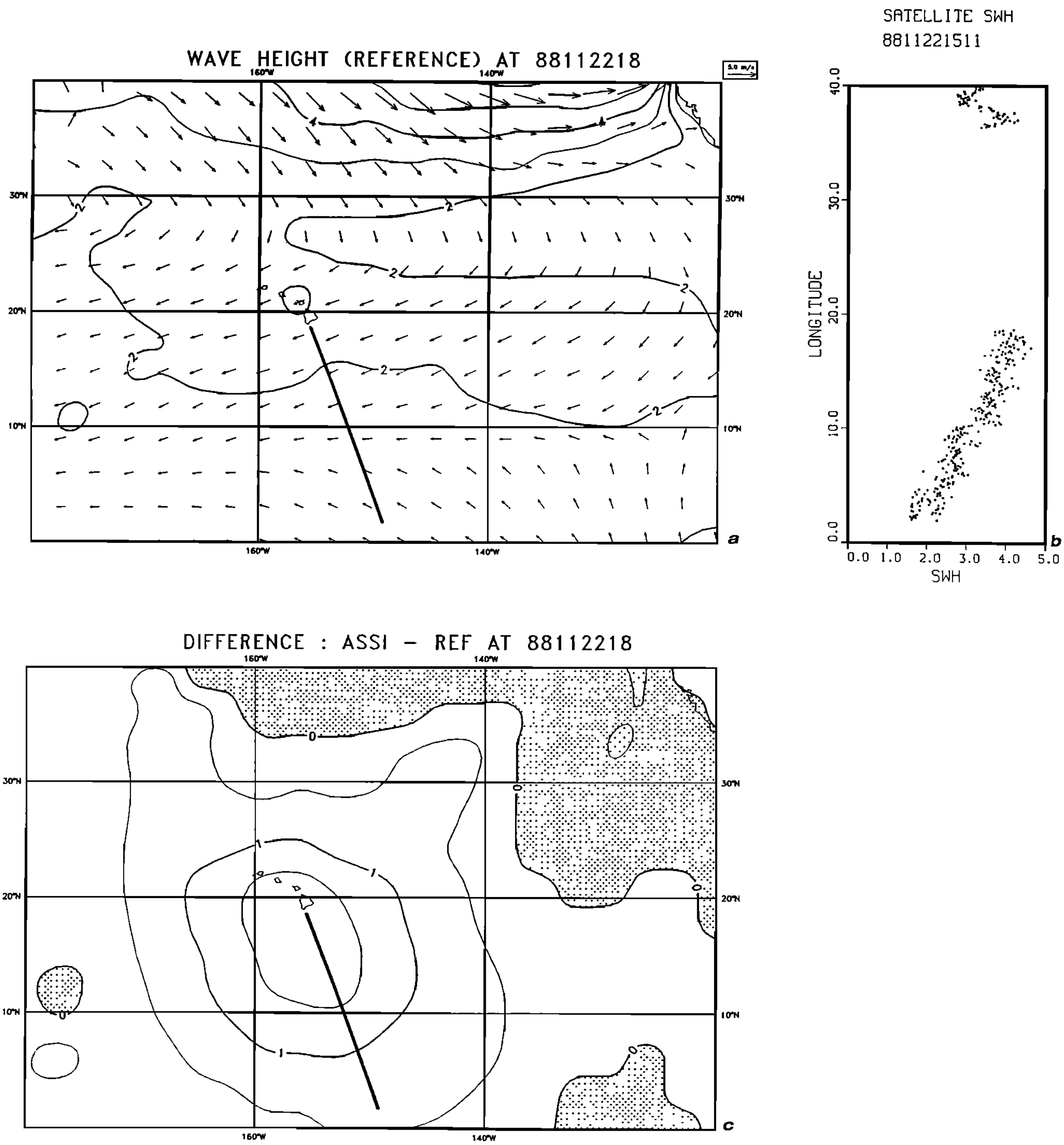

Fig. 23. (*a*) SWH field near Hawaii with the satellite track on November 22 at 18 UT. (*b*) Altimeter SWH data along the satellite tracks (the approximate time of the passage is displayed; read 8811221511 as November 22, 1988, 1511 UT). (*c*) Differences between assimilation run and reference run.

6. Conclusions

With respect to the results of the study by *Janssen et al.* [1989], an improvement has been achieved. In fact, benefits are larger and they persist longer. This can be explained by the different approach used to update the swell [see *Lionello et al.*, 1991], by the use of the OI to create analyzed fields, and by the accurate fit to the model growth which improves the evaluation of the surface stress. The benefits are particularly evident from statistics of model results against altimeter data, which show a positive impact of the assimilation.

It appears that analyses of swell and of wind sea produce quantitatively comparable benefits. Therefore methods that select only wind sea or swell updating are not capable of fully exploiting the satellite data. In fact, the improvement due to the updating of swell may have a longer memory than that derived by updating the wind sea, but in the presence of

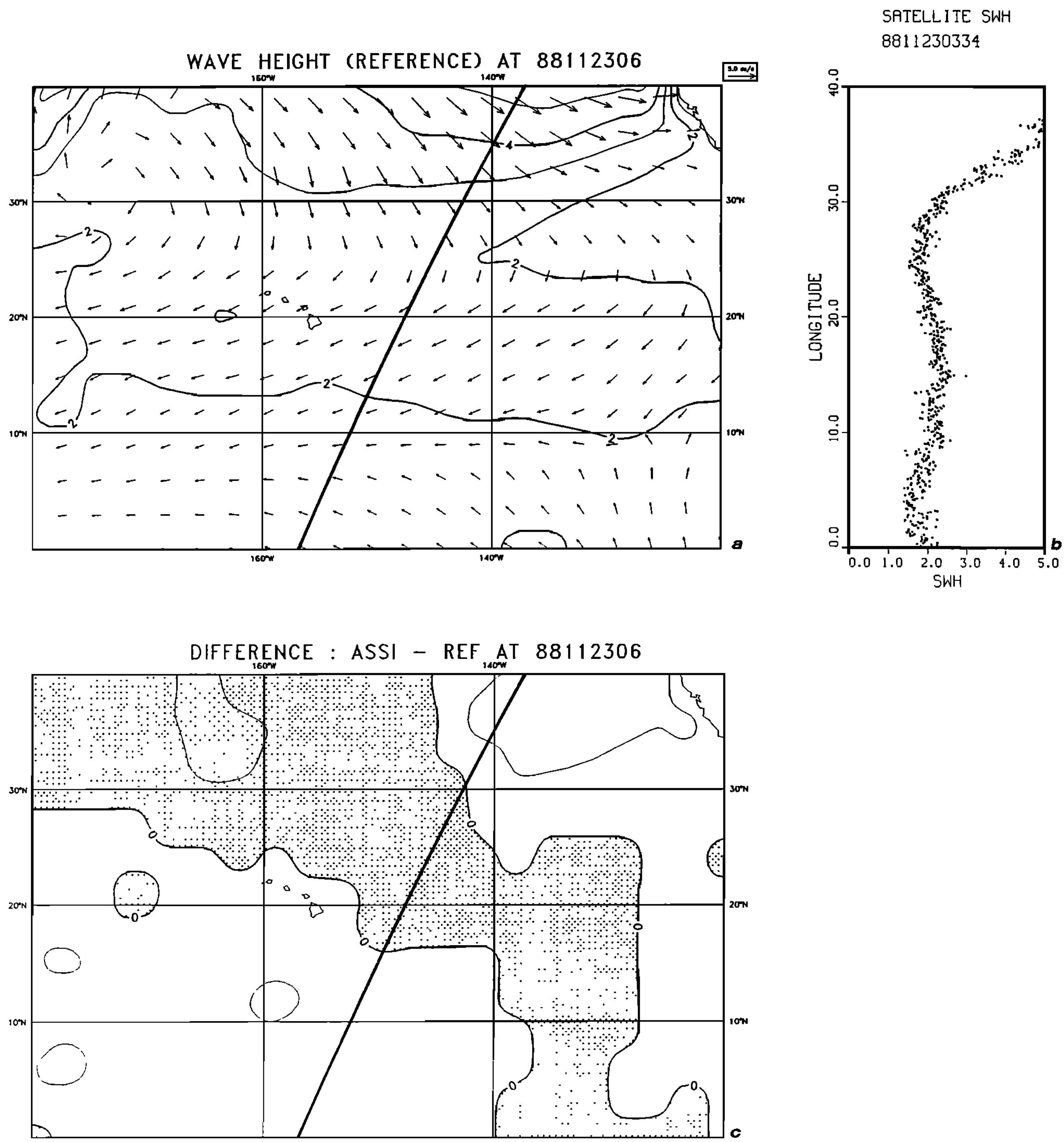

Fig. 24. (*a*) SWH field near Hawaii with the satellite track on November 23 at 6 UT. (*b*) Altimeter SWH data along the satellite track (the approximate time of the passage is displayed). (*c*) Differences between assimilation run and reference run.

large storm systems, which are the most interesting cases, as in the southern ocean, the updating of the wind sea has a comparable or larger impact.

As anticipated, it is obvious that a wave model loses the memory of the correction because as soon the assimilation stops, the forcing tends to erase its effect. In this respect a longer-lasting effect can be obtained only if the estimate of the surface stress, derived by analyzing the wave field, is used by the analysis in the atmospheric model, having an effect in the wind fields that are successively used.

It must be observed that in many cases the corrections are not dramatic, showing a substantial agreement of WAM model and satellite measurements; consequently, no very large modifications of the stress fields are required in most of the cases, but when there is a more substantial disagreement (for instance in the storms in the southern ocean during the

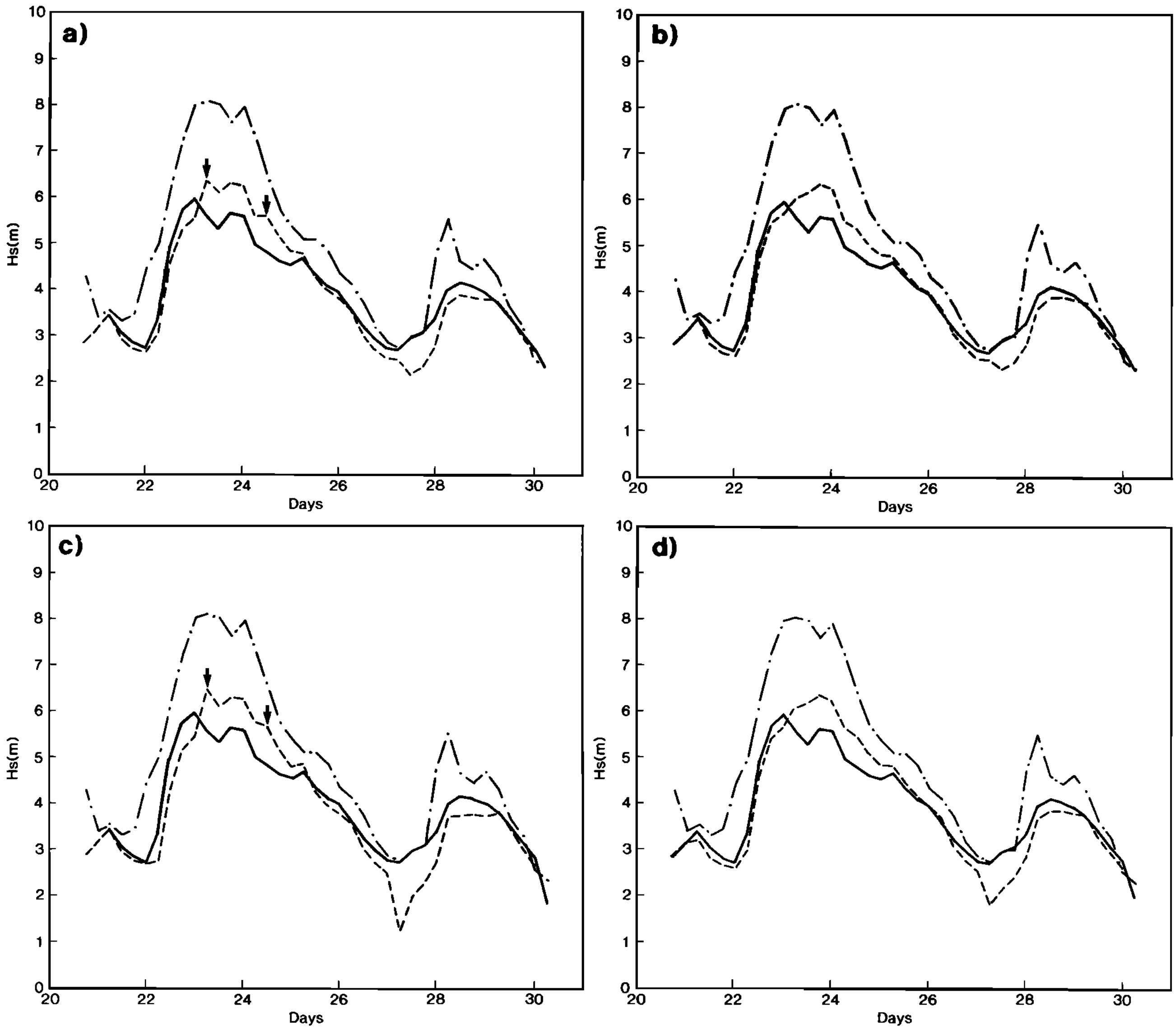

Fig. 25. SWH time series at buoy 46002. Dash-dot lines indicate buoy measurements; solid lines, reference experiment; and dashed lines, assimilation experiments. Each figure shows a different data assimilation experiment: (*a*) $L_{max} = 3$, $R = 0$; (*b*) $L_{max} = 3$, $R = 1$; (*c*) $L_{max} = 5$, $R = 0$; (*d*) $L_{max} = 5$, $R = 1$.

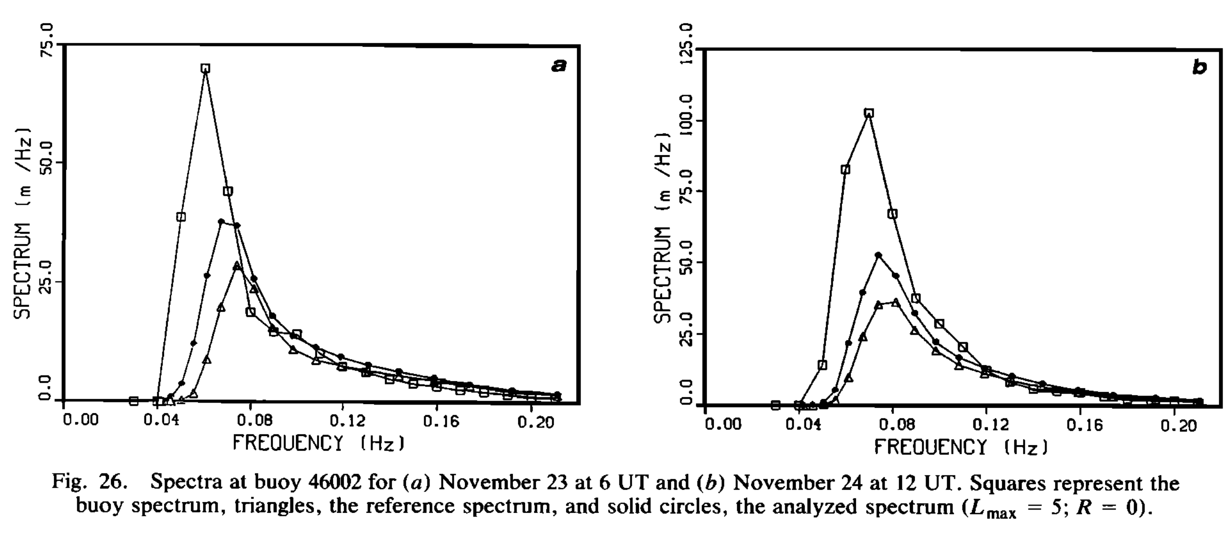

Fig. 26. Spectra at buoy 46002 for (*a*) November 23 at 6 UT and (*b*) November 24 at 12 UT. Squares represent the buoy spectrum, triangles, the reference spectrum, and solid circles, the analyzed spectrum ($L_{max} = 5$; $R = 0$).

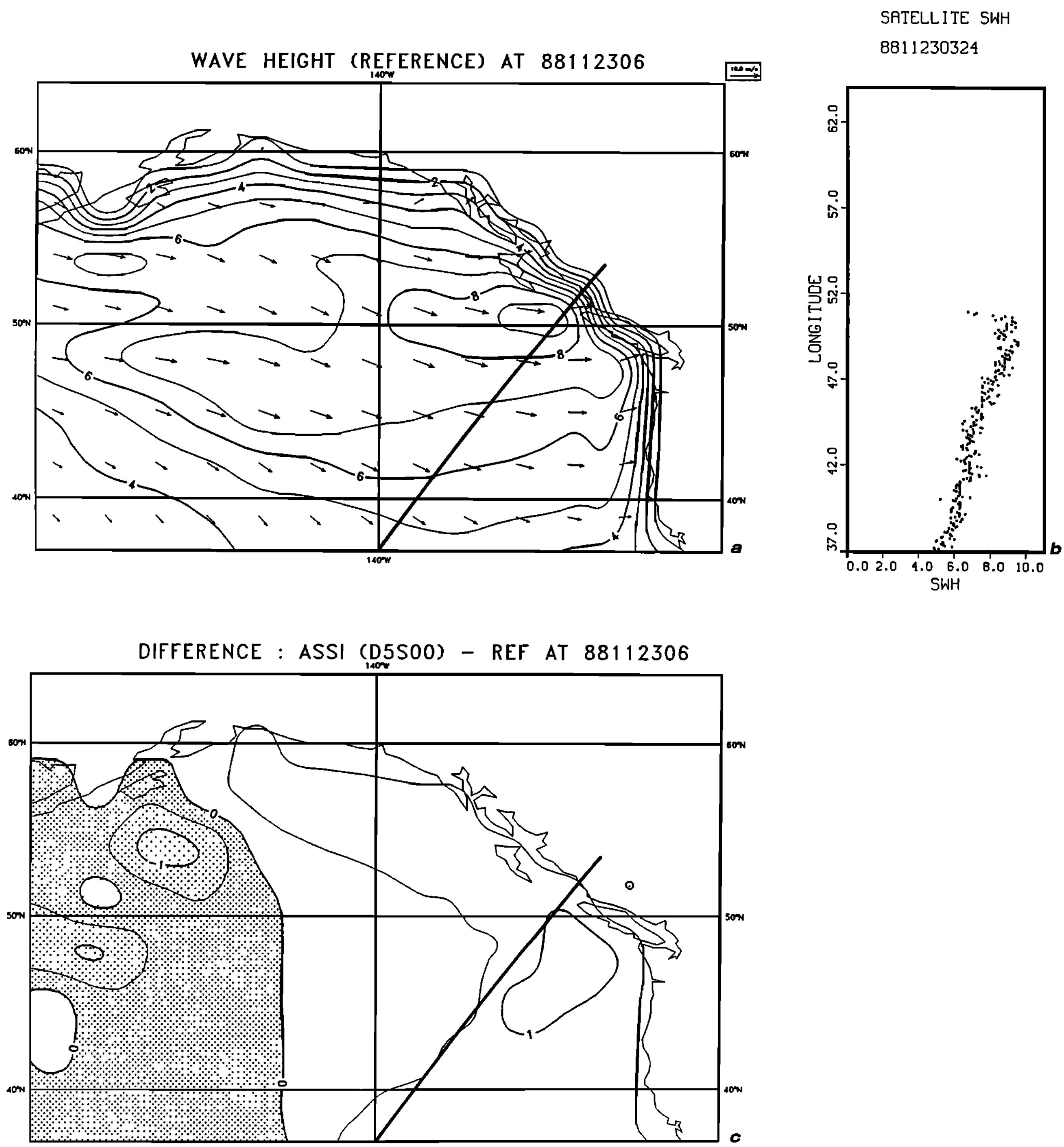

Fig. 27. (*a*) SWH field in the Gulf of Alaska with the satellite track on November 23 at 6 UT. (*b*) altimeter SWH data along the satellite track (the approximate time of the passage is displayed). (*c*) Differences between assimilation run and reference run.

Seasat experiment), the analysis of the wave field has a substantial impact on the stress field.

The conclusions from the comparison with the buoy observations are uncertain because of some apparent inconsistency between buoy and altimeter data. In fact, the generally fair agreement of WAM model reference run and altimeter data is surprising because of the many peak events that were recorded by buoys and that were not reproduced by the WAM model. In the cases that we specifically examined, the results suggest that the altimeter did not detect the extreme events recorded by the buoys in the Gulf of Alaska, and their recovery with the assimilation was therefore impossible. Consequently, while at Hawaii both the results presented in sections 4 and 5 show the same dependence on $L_{\max}$, the trend is not confirmed in the Gulf of Alaska.

There are two possible explanations. The first possibility is that for extreme waves the altimeter is systematically

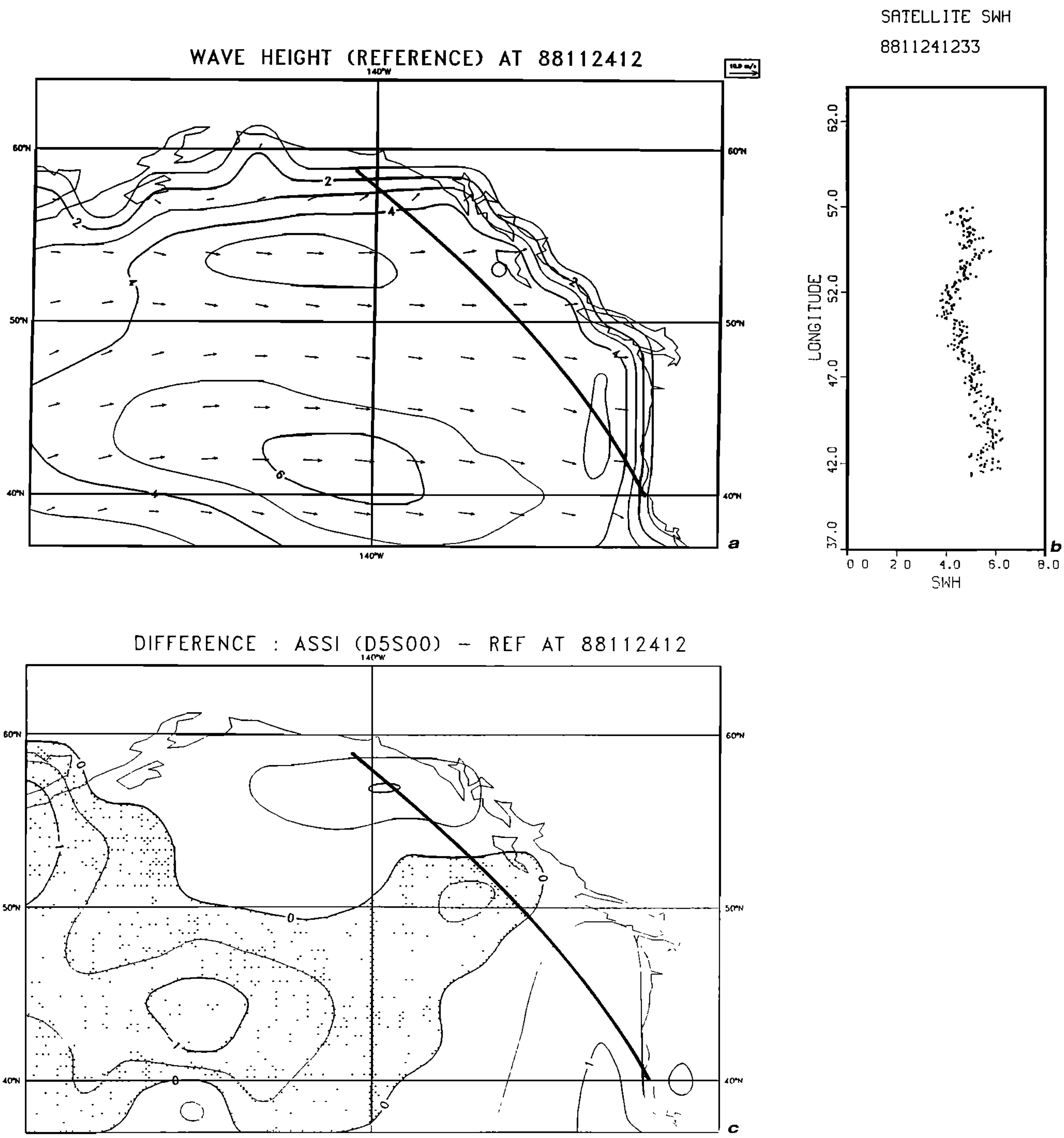

Fig. 28. (*a*) SWH field in the Gulf of Alaska with the satellite track on November 24 at 12 UT. (*b*) Altimeter SWH data along the satellite track (the approximate time of the passage is displayed). (*c*) Differences between assimilation run and reference run.

biased low with respect to buoys. The second is that local features, not detected by the satellite and absent in the WAM model results, were present. If this were the case, then the solution would require more data, i.e., eventually more satellites.

The analysis has provided useful indications of the shortcomings of the wave model: in spite of a tendency to overevaluate the wind sea, there is a tendency to underevaluate the swell. Some disappointing results may be due to problems in the wave model which cannot propagate adequately an energy initially correctly located in the exact amount. Clearly, the assimilation scheme cannot compensate a wrong propagation of the information. Actually, the first-order propagation scheme that is implemented in the WAM model is likely to produce an excessive diffusion of the wave energy decreasing the effectiveness of the assimilation or misplacing the correction introduced by the assimilation. This could be avoided by using a higher-order propagation scheme including an explicit diffusion term [*WAMDI Group*, 1988]. An incorrect dissipation source function can be blamed as well. In fact, the WAM model dissipation source function has been tuned to reproduce the Pierson-Moskowitz spectrum as a final stage of the wave growth. Its extension to the physically completely different situation of the wind sea decay is arbitrary, and possibly a different expression should be used in this case. Also this systematic flaw, which cannot be compensated by the assimilation, tends to reduce its effectiveness.

It is clear from this study that the utility of satellite data for wave modeling is not only in the possibility of correcting the model. Because of the wide coverage that they offer, they are a very useful tool to point out the shortcomings of a wave model. This opportunity will be greatly increased by the availability of SAR data and of an efficient algorithm to invert the SAR image. On the other hand, by the cross validation with other data sources, wave models offer the possibility of investigating the weak points of satellite measurements.

Acknowledgments. We are indebted to Tony Hollingsworth for discussions during our stay at ECMWF. Liana Zambresky gave us the data and the software that she used for a verification study with the WAM model. We thank the GKSS Forschungszentrum for having supplied the Geosat data. Finally, the user supporters of ECMWF, Norbert Kreitz and John Greenaway, have been a great help.

REFERENCES

Anderson, D., A. Hollingsworth, S. Uppala, and P. Woicheshyn, A study on the feasibility of using sea and wind information from the ERS-1 satellite, I, Wind scatterometer data, ECMWF contract report, Eur. Space Agency, Paris, 1987.

Brüning, C., W. Alpers, and K. Hasselmann, Monte Carlo simulation studies of the nonlinear imaging of a two dimensional surface wave field by a syntetic aperture radar, *Int. J. Remote Sens.*, *11*(10), 695–727, 1990.

de Valk, C. F., and C. J. Calkoen, Wave data assimilation in a third generation wave prediction model for the North Sea, report, Delft Hydraul. Lab., Delft, Netherlands, 1989.

Esteva, D. C., Evaluation of preliminary experiments assimilating Seasat significant wave heights into a spectral wave model, *J. Geophys. Res.*, *93*, 14,099–14,106, 1988.

Francis, P. E., and R. A. Stratton, Some experiments to investigate the assimilation of Seasat altimeter wave height data into a global wave model, *Q. J. R. Meteorol. Soc.*, *116*, 1225–1251, 1990.

Hasselmann, K., et al., Measurements of wind-wave growth and swell decay during the Joint North Sea Wave Project (JONSWAP), *Dtsch. Hydrogr. Z.*, *8*(12), suppl. A, 95 pp., 1973.

Hasselmann, K., S. Hasselmann, E. Bauer, C. Brüning, S. Lehner, H. Graber, and P. Lionello, Development of a satellite SAR image spectra and altimeter wave height data assimilation system for ERS-1, *Rep. 19*, 157 pp., Max-Planck-Inst. für Meteorol., Hamburg, Germany, 1988.

Hollingsworth, A., Objective analysis for numerical weather prediction, *J. Meteorol. Soc. Jpn.*, WMO/IUGG/MWP Symp. spec. issue, 11–60, 1986.

Janssen, P. A. E. M., P. Lionello, M. Reistad, and A. Hollingsworth, Hindcasts and data assimilation studies with the WAM model during the Seasat period, *J. Geophys. Res.*, *94*, 973–993, 1989.

Kitaigorodskii, S. A., Application of the theory of similarity to the analysis of wind-generated water waves as a stochastic process, *Bull. Acad. Sci. USSR Geophys. Ser.*, no. 1, 73 pp., 1962.

Lionello, P., and P. A. E. M. Janssen, Assimilation of altimeter measurements to update swell spectra in wave models, paper presented at the International Symposium on Assimilation of Observations in Meteorology and Oceanography, World Meteorol. Organ., Clermond-Ferrand, France, Aug. 1990.

Lionello, P., H. Günther, and P. A. E. M. Janssen, Assimilation of altimeter data in a global third generation wave model, technical report, Eur. Cent. for Med. Range Weather Forecasts, Reading, England, 1991.

Thomas, J., Retrieval of energy spectra from measured data for assimilation into a wave model, *Q. J. R. Meteorol. Soc.*, *114*, 781–800, 1988.

WAMDI Group (S. Hasselmann et al.), The WAM model—A third generation ocean wave prediction model, *J. Phys. Oceanogr.*, *18*, 1776–1810, 1988.

Zambresky, L., A verification study of the global WAM model, *Tech. Rep. 63*, Res. Dep., Eur. Cent. for Med. Range Weather Forecasts, Reading, England, 1988.

H. Günther, Forschungszentrum GKSS, Geesthacht, Postfach 1160, 2054 Geesthacht, Germany.

P. A. E. M. Janssen, Koninklijk Nederlands Meteorologisch Institut, P.O. Box 201, 3730 AE de Bilt, Netherlands.

P. Lionello, Instituto per lo Studio della Dinamica delle Grandi Masse, CNR, 1364 San Polo, 30125 Venezia, Italy.

(Received August 28, 1991;
revised December 24, 1991;
accepted February 7, 1992.)